Advantages of diffuse radiation for terrestrial ecosystem productivity

Lianhong Gu,[1] Dennis Baldocchi,[1] Shashi B. Verma,[2] T. A. Black,[3] Timo Vesala,[4] Eva M. Falge,[5] and Pete R. Dowty[6,7]

Received 8 August 2001; revised 19 October 2001; accepted 21 October 2001; published 29 March 2002.

[1] Clouds and aerosols alter the proportion of diffuse radiation in global solar radiation reaching the Earth's surface. It is known that diffuse and direct beam radiation differ in the way they transfer through plant canopies and affect the summation of nonlinear processes like photosynthesis differently than what would occur at the leaf scale. We compared the relative efficiencies of canopy photosynthesis to diffuse and direct photosynthetically active radiation (PAR) for a Scots pine forest, an aspen forest, a mixed deciduous forest, a tallgrass prairie and a winter wheat crop. The comparison was based on the seasonal patterns of the parameters that define the canopy photosynthetic responses to diffuse PAR and those that define the responses to direct PAR. These parameters were inferred from half-hourly tower CO_2 flux measurements. We found that: (1) diffuse radiation results in higher light use efficiencies by plant canopies; (2) diffuse radiation has much less tendency to cause canopy photosynthetic saturation; (3) the advantages of diffuse radiation over direct radiation increase with radiation level; (4) temperature as well as vapor pressure deficit can cause different responses in diffuse and direct canopy photosynthesis, indicating that their impacts on terrestrial ecosystem carbon assimilation may depend on radiation regimes and thus sky conditions. These findings call for different treatments of diffuse and direct radiation in models of global primary production, and studies of the roles of clouds and aerosols in global carbon cycle. *INDEX TERMS:* 4806 Oceanography: Biological and Chemical: Carbon cycling; 0315 Atmospheric Composition and Structure: Biosphere/atmosphere interactions; 1851 Hydrology: Plant ecology; 1610 Global Change: Atmosphere (0315, 0325); *KEYWORDS:* diffuse and direct PAR, terrestrial ecosystem productivity, clouds, aerosols, global carbon cycle

1. Introduction

[2] A plant canopy consists of an assemblage of plants, whose leaves possess a particular spatial distribution and assortment of angle orientations [*de Wit*, 1965; *Monsi and Saeki*, 1953]. How a collection of leaves intercepts sunlight and uses light energy to assimilate carbon dioxide (CO_2) is the basis of canopy photosynthesis. The radiation environment inside a plant canopy is dynamic in both time and space (vertically as well as horizontally), owing to temporal changes in the solar elevation angle, the presence of clouds, the motion of the canopy, and spatial variations in plant canopy physical structure and physiological capacity. Interacting with this dynamic radiation environment are several vertical biological and environmental gradients within plant canopies, including profiles of leaf nitrogen content, photosynthetic capacity, temperature, humidity, wind speed, CO_2 concentration, etc. These canopy structure-induced complexities can lead to emergent properties that are not expected from photosynthesis of a single leaf. One such example is the differentiation in impacts of diffuse and direct photosynthetically active radiation (PAR) on canopy photosynthesis.

[3] Crop scientists have long realized that radiation-use efficiency (RUE, defined as the ratio between grams of biomass accumulated and total solar radiation intercepted) or light use efficiency (LUE, similar to RUE, but based on PAR only) is higher for diffuse radiation than for direct radiation [*de Wit*, 1965; *Allen et al.*, 1974; *Goudriaan*, 1977; *Norman*, 1980; *Norman and Arkebauer*, 1991; *Sinclair et al.*, 1992; *Sinclair and Shiraiwa*, 1993; *Rochette et al.*, 1996; *Healey et al.*, 1998]. *Sinclair et al.* [1992] speculated that higher diffuse RUE might explain why some crop species growing under glasshouses show higher RUE than those growing in open fields. However, they did not quantitatively compare the inside radiation with the outdoor environment. *Young and Smith* [1983] reported that an understory herb in a mixed spruce stand gained more carbon on representative cloudy days than on clear days. They suggested that this could be due to greater diffuse PAR flux density and increased plant water potentials under cloudy sky conditions. With increasing interests in terrestrial ecosystem carbon sequestration and new technologies available for measuring fluxes over tall canopies [*Verma et al.*, 1986; *Baldocchi et al.*, 1988], observational studies on the relationship between the radiation environment and CO_2 exchange of forests became possible. Numerous researchers have since reported significantly higher radiation use efficiencies during cloudy days than during clear days for both coniferous and deciduous forests [*Price and Black*, 1990; *Hollinger et al.*, 1994; *Fan et al.*, 1995; *Fitzjarrald et*

[1]Ecosystem Science Division, Department of Environmental Science, Policy and Management, University of California, Berkeley, California, USA.
[2]School of Natural Resource Sciences, University of Nebraska, Lincoln, Nebraska, USA.
[3]Faculty of Agricultural Sciences, University of British Columbia, Vancouver, British Columbia, Canada.
[4]Department of Physical Sciences, University of Helsinki, Helsinki, Finland.
[5]Department of Plant Ecology, University of Bayreuth, Bayreuth, Germany.
[6]Department of Environmental Sciences, University of Virginia, Charlottesville, Virginia, USA.
[7]Now at Puget Sound Water Quality Action Team, Office of the Governor, Olympia, Washington, USA.

0148-0227/02/2001JD001242$09.00

al., 1995; *Sakai et al.*, 1996; *Baldocchi*, 1997; *Baldocchi et al.*, 1997; *Goulden et al.*, 1997; *Lamaud et al.*, 1997; *Freedman et al.*, 1998; *Gu et al.*, 1999; *Freedman et al.*, 2001]. Typically, this is shown by the alienation of light responses of net ecosystem exchange (NEE) of CO_2 between clear and cloudy days with cloudy days having a higher NEE rate (in terms of the absolute value) than clear days for the same solar irradiance level.

[4] It is important to compare RUE, or LUE, at the same irradiance level because both variables decrease with increasing irradiance level due to light saturation effect. A somewhat unexpected finding reported by some of these studies is that the highest rate of forest NEE of CO_2 (that is, the most negative value, following the NEE sign convention) often occurs on cloudy rather than on sunny days even through solar radiation is substantially lower on cloudy days than on sunny days [*Price and Black*, 1990; *Hollinger et al.*, 1994; *Fitzjarrald et al.*, 1995; *Sakai et al.*, 1996; *Freedman et al.*, 1998; *Gu et al.*, 1999; *Freedman et al.*, 2001]. *Gu et al.* [1999] showed that the maximum carbon sequestration by two temperate forest ecosystems happened under sky conditions with a solar radiation level equivalent to about 70–80% of clear-sky solar irradiance and clouds reduced the solar irradiance by as much as 50% without lowering the capacity of these two forests in carbon sequestration as compared with clear days. Except for a few cases [e.g., *Freedman et al.*, 1998, 2001], most of these studies used changes in surface solar irradiance as a measure of cloudiness and did not actually conduct cloud observations.

[5] Clouds reduce the global solar radiation but increase the relative proportion of diffuse radiation at the Earth surface. A critical aspect of cloud modulation of surface solar radiation is that clouds can also increase the absolute amount of diffuse radiation if the sky is not too cloudy [*Gu et al.*, 1999]. Because of the higher RUE of diffuse radiation, clouds can actually enhance terrestrial ecosystem carbon assimilation if the photosynthetic gains of increased diffuse radiation exceed the photosynthetic losses of reduced direct beam radiation. This line of reasoning has led some researchers to use increased diffuse radiation to explain enhanced ecosystem carbon sequestration under cloudy sky conditions [*Price and Black*, 1990; *Hollinger et al.*, 1994; *Fan et al.*, 1995; *Goulden et al.*, 1997]. However, it should be pointed out that increased diffuse radiation might not be the only factor responsible for the enhanced ecosystem carbon assimilation observed under cloudy sky conditions [*Young and Smith*, 1983; *Baldocchi*, 1997; *Gu et al.*, 1999]. In addition to changes in surface solar radiation, the presence of clouds can be both causes and consequences of changes in many atmospheric factors such as temperature, moisture, and latent heating, precipitation, etc. These factors all have direct or indirect influences on terrestrial ecosystem carbon assimilation [*Gu et al.*, 1999]. Therefore some researchers emphasized decreases in the respiration of sunlit leaves due to reduced leaf temperature [*Baldocchi*, 1997], reduction in vapor pressure deficit (VPD) [*Freedman et al.*, 1998, 2001], stomatal dynamics associated with light fluctuations [*Fitzjarrald et al.*, 1995; *Sakai et al.*, 1996]. We may also expect that sparse and dense canopies behave differently. Under a sparse canopy, much solar radiation can reach the soil, heat it, and promote soil respiration, resulting in reduced net ecosystem carbon uptake on clear days. Because of these considerations, *Gu et al.* [1999] stressed the multiplicity of environmental factors influencing ecosystem carbon sequestration under cloudy conditions. In this paper, however, we focus on detecting the differences in the effects of diffuse and direct radiation.

[6] Much understanding on the canopy differential responses to diffuse and direct radiation has been gained from numerous canopy photosynthesis models [e.g., *de Wit*, 1965; *Allen et al.*, 1974; *Goudriaan*, 1977; *Norman*, 1980; *Ross*, 1981; *Jarvis et al.*, 1985; *Wang and Jarvis*, 1990; *Gutschick*, 1991; *Norman and Arkebauer*, 1991; *Sinclair et al.*, 1992; *Sinclair and Shiraiwa*, 1993; *De Pury and Farquhar*, 1997; *Baldocchi*, 1997; *Choudhury*, 2000; *Choudhury*, 2001a, 2001b]. Although it is a general agreement among these models that canopy RUE is higher for diffuse radiation than for direct radiation, different models may have different sensitivities on the separation of diffuse and direct radiation for predicting canopy photosynthetic productivities. For example, the model of *de Wit* [1965] showed only a slight dependence of RUE on the fraction of diffuse radiation, which led *de Wit* [1965 p. 37] to conclude "it is not worthwhile to spend much energy on measuring the fraction of diffuse light in order to improve on the calculation of photosynthesis." On the contrary, the model of *Goudriaan* [1977] sensitively depended on the separation of diffuse and direct radiation for canopy photosynthesis, and the author stated that "separate measurements of diffuse and direct radiation are almost as important as measuring the total solar radiation" [*Goudriaan*, 1977, p. 192]. Considering the complexities involved in predicting canopy photosynthesis, this type of disagreement is not surprising, especially for early models. With better understanding and quantitative treatments in canopy radiative transfer, leaf photosynthesis, transpiration, stomatal conductance, energy balance, etc., more recent models generally reveal high sensitivities of canopy photosynthesis to the fraction of diffuse radiation [*Jarvis et al.*, 1985; *Wang and Jarvis*, 1990; *Gutschick*, 1991; *Norman and Arkebauer*, 1991; *Sinclair et al.*, 1992; *Sinclair and Shiraiwa*, 1993; *De Pury and Farquhar*, 1997; *Choudhury*, 2000; *Choudhury*, 2001a, 2001b]. *Norman and Arkebauer* [1991] used the Cupid model to show that canopy LUE increases nearly linearly with the fraction of diffuse PAR. Using a different model, *Choudhury* [2000, 2001a, 2001b] came to similar conclusions. According to the predictions of these studies, LUE of diffuse PAR can be several times higher than LUE of direct PAR.

[7] The sensitive dependence of canopy photosynthesis on the fraction of diffuse radiation as revealed by modern biophysical canopy models is apparently in consensus with the scenario that uses enhanced diffuse radiation to explain field observation of significantly higher RUE on cloudy days than on clear days. However, experimental studies, which go beyond simple comparisons between cloudy and clear days and directly address the canopy photosynthetic differences between diffuse and direct radiation, are still needed. This is important since a variety of environmental factors can differ and no conclusive statements can be made on which factors are responsible for the differences in light response curves between cloudy and clear days. *Gu et al.* [1999] elaborated this point.

[8] Conceptually, the differences of canopy photosynthetic responses to diffuse and direct PAR are relatively easy to understand. They result from the differences in diffuse and direct radiative transfer regimes in plant canopies coupled with the nonlinearity of photosynthesis. While the irradiance from the diffuse skylight on all leaves at a given canopy depth is nearly the same [*Gutschick*, 1991], the irradiance on sunlit leaves, which are illuminated by both the direct beam and diffuse radiation and represent only a fraction of all leaves in the canopy, ranges from the level of a shaded leaf to full light, depending on the angles between leaf orientation and beam propagation direction. Meanwhile, as the irradiance level increases, leaf photosynthesis shifts from RuBP regeneration (electron transport) limitation to Rubisco (CO_2 diffusion) control [*Farquhar et al.*, 1980]. This leads to photosynthetic saturation and decrease in RUE under high irradiance levels. Therefore the transfer regime of direct beam radiation wastes photons by concentrating the light resource to only a fraction of all leaves, leading to a less efficient photosynthetic use of light by plant canopies. Diffuse radiation, however, effectively avoids the light saturation constraint by more evenly distributing radiation among all leaves in plant canopies, and leads to a more efficient use of light.

[9] A closely related issue is the necessity of separating leaves into sunlit and shaded groups to predict canopy photosynthesis. This has been well recognized by terrestrial ecosystem biophysical

Table 1. Locations, Climates, and Vegetative and Edaphic Characteristics of the Five Sites Investigated in This Study[a]

	Scots Pine Forest	Aspen Forest	Tallgrass Prairie	Mixed Forest	Wheat
Location	61°51′N, 24°17′E, Finland	53°63′N, 106°20′W, Canada	36°56′N, 96°41′W, United States	35°58′N, 84°17′W, United States	36°46′N, 97°08′W, United States
Mean annual temperature, °C	3	1	15	13.9	15
Annual precipitation, mm	700	400	1103	1372	1044
Canopy height, m	13	22	0.6 at maximum	26	0.9 at maximum
Stand age	35	70		55	
Maximal LAI	9.0	4.5	3.0	4.9	5.0
Stem density or basal area	2500 stem ha^{-1}	830 stem ha^{-1}		23 m^2 ha^{-1}	
Dominant species	*Pinus sylvestris L.*	*Populus tremuloides Michx. Corylus cornuta* (understory)	little bluestem, blue grama, big bluestem, Indiangrass, poverty dropseed	*Q prinus L., Q alba L., Acer rubrum L., A. saccharum, Liriodendron tulipifera, Carya sp.*	winter wheat
Soil type	Haplic Podzol, coarse, silty, glacial till	Orthic Luvisol, silty-clay texture	silty clay loam of Wolco-Dwight complex (thermic Pachic Argiustolls and mesic Typic)	Fullerton cherty silt loam (Typic Paleudult)	silty clay loam of Poncreek and Kirkland complexes (Typic and Pachic Argiustolls)

[a] Data from 1997 at the Scots pine forest, tallgrass prairie, and winter wheat crop sites, 1996 at the aspen forest site, and 1995 at the mixed deciduous forest site are used in the analyses.

modeling communities [*Sinclair et al.*, 1976; *Norman*, 1980; *Wang and Jarvis*, 1990; *Wang et al.*, 1992; *De Pury and Farquhar*, 1997; *Baldocchi*, 1997; *Wang and Leuning*, 1998]. The distribution of sunlight in canopies is bimodal: most leaves are shaded with low-intensity light or sunlit with high-intensity light. Few if any are exposed to the mean light level. The light responses of the groups of shaded and sunlit leaves are distinctively different from each other. The light response for the group of sunlit leaves quickly saturates with increasing light level because the light is concentrated among a relatively small number of leaves. Further increase in radiation can even lead to decreases in photosynthesis because of elevated temperature and enhanced respiration. In contrast, the light response curve for the group of shaded leaves is very linear as the light is shared by a relatively large amount of leaves and each leaf tends to inhabit the linear portion of the leaf-level light response curve [*Baldocchi*, 1997]. Therefore proper treatment of these two groups of leaves is important for accurately predicting canopy photosynthesis. To determine the fractions of sunlit and shaded leaves in a canopy, one needs to deal with the issue of leaf clumping as natural canopies often have leaves clumped, which can have significant effects on canopy photosynthesis [*Baldocchi and Wilson*, 2001].

[10] However, the issues of separating leaves into sunlit and shaded groups and incident solar radiation into direct and diffuse components are not identical. Without separating sunlit from shaded leaves, canopy photosynthesis is overestimated [*Spitters*, 1986; *De Pury and Farquhar*, 1997, 1999; *Wang and Leuning*, 1999] because the effects of light saturation (in the case of sunlit leaves) and light constraint (in the case of shaded leaves) cannot be captured by such schemes. In contrast, failure to partition incident solar radiation into diffuse and direct components by treating the global radiation as direct beam radiation will lead to underestimating canopy photosynthesis, especially under cloudy conditions, because the higher diffuse radiation use efficiency is missed [*Gu et al.*, 1999]. Therefore it is desirable for biophysical canopy models to do both separations properly. However, models that address only one of these two issues but not both are likely to perform worse than models that address none of them due to their opposite impacts on canopy photosynthesis estimation.

[11] Although the underlying mechanism for the differentiation in impacts of diffuse and direct PAR on canopy photosynthesis has been understood quite well, quantifying this differentiation from measurements is difficult and can only be done indirectly. This is because solar radiation at the Earth surface is always composed of diffuse and direct PAR simultaneously even on sunshine or overcast days. Further complicating this issue is that a variety of environmental factors, in addition to diffuse and direct radiation, can change with sky conditions. Thus complete pictures of canopy photosynthetic responses to diffuse PAR or direct PAR cannot be obtained directly under natural conditions. To overcome this problem, new analysis approaches are needed. To our knowledge, there have been no systematic analyses on the behaviors of canopy photosynthetic responses to diffuse or direct PAR based on field flux measurements in the literature. However, large-scale models such as regional or global gross primary production (GPP) models often rely on our quantitative understandings of canopy photosynthesis derived from light response curves. For example, many GPP models use LUE modulated by environmental stress functions to predict primary productivity [*Monteith*, 1977; *Prince*, 1991; *Law and Waring*, 1994; *Runyon et al.*, 1994; *Ruimy et al.*, 1994; *Landsberg et al.*, 1995; *Prince and Goward*, 1995; *Ruimy et al.*, 1995]. Currently, GPP models rarely implement different LUEs for diffuse and direct PAR in their algorithms with only a few exceptions that rely on results from canopy biophysical models [*Anderson et al.*, 2000; *Choudhury*, 2000, 2001a, 2001b; *Roderick et al.*, 2001]. A quantitative understanding of the differences in the behaviors of canopy photosynthesis between diffuse and direct PAR that is supported directly by field flux observations is much needed.

[12] There are three main objectives in this paper: (1) to introduce a method for inferring canopy photosynthetic characteristics of both diffuse and direct PAR from tower flux measurements; (2) to use the developed method to test the previous modeling finding of the advantages of diffuse PAR by evaluating the differences in canopy photosynthetic effects between diffuse and direct PAR for a Scots pine forest, a mixed deciduous forest, an aspen forest, a tallgrass prairie, and a winter wheat crop; and (3) to examine differences, similarities, and environmental controls in canopy photosynthetic characteristics of diffuse and direct PAR for these ecosystems. To achieve these objectives, we take advantage of long-term tower flux measurements at these sites. We base our analyses on the seasonal dynamics of characteristic canopy photosynthetic parameters for diffuse and direct PAR derived from flux measurements. The

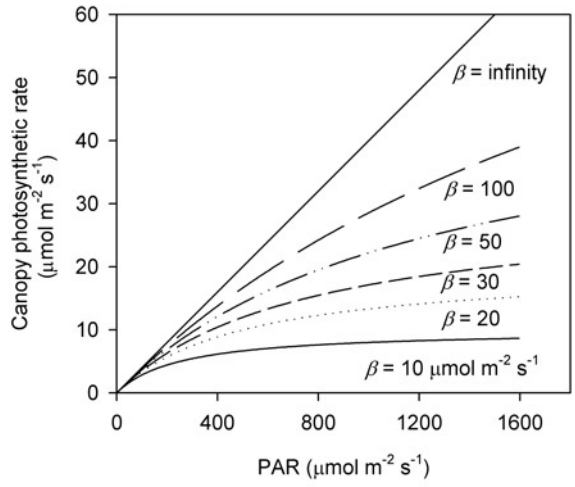

Figure 1. Effects of the parameter β in the rectangular hyperbola (equation (2)) on the response of canopy photosynthesis to the incident PAR.

findings presented in this paper will provide a basis for global GPP models to apply different treatments for diffuse and direct PAR in their algorithms.

2. Sites and Measurements

[13] This study was conducted at five sites: a Scots pine forest in Finland, an aspen forest in Canada, a mixed deciduous forest, a native tallgrass prairie, and a cultivated winter wheat crop in the United States (Table 1). We selected these five locations from the tower sites in the FLUXNET project (http://public.ornl.gov/FLUXNET/) [*Running et al.*, 1999; *Baldocchi et al.*, 2001] to cover a broad vegetation spectrum and climate conditions. Table 1 summarizes locations, climate conditions, and vegetative and edaphic characteristics of these five sites.

[14] The data from the Scots pine forest were collected at the Station for Measuring Forest Ecosystem-Atmosphere Relations (SMEAR II) field measurement station, which is located in Hyytiälä, southern Finland [*Vesala et al.*, 1998]. The stand is homogeneous for about 200 m in all directions from the measurement site, extending to the north for about 1.2 km (60° sector). The terrain is subject to modest height variation. An eddy covariance (EC) system, which included an ultrasonic anemometer and a closed-path infrared gas analyzer, was installed to measure the net ecosystem CO_2 exchange at 23 m above the ground (10 m above the canopy). Detailed descriptions on the site conditions, the setup of the eddy covariance system, and the microclimate measurements have been given elsewhere [*Vesala et al.*, 1998; *Rannik*, 1998; *Rannik and Vesala*, 1999; *Rannik et al.*, 2000].

[15] Located in the southern part of Prince Albert National Park, Saskatchewan, Canada, the aspen forest site was in a horizontally extensive and homogeneous even-aged stand. This mature aspen forest was regenerated after a natural fire in 1919 [*Weir*, 1996]. Half-hourly fluxes of CO_2 were measured using the EC technique at 39.5 m above the ground (17.5 m above the canopy, see Table 1). The EC sensors consisted of a three-dimensional sonic anemometer and a closed-path infrared gas analyzer [*Chen et al.*, 1999]. For detailed information on the site and measurements, readers are referred to *Black et al.* [1996], *Blanken et al.* [1997], *Chen et al.* [1999], and *Black et al.* [2000].

[16] The mixed deciduous forest site is located at the Walker Branch Watershed in eastern Tennessee. This forest has regenerated from agricultural land. The EC instruments, which included a three-dimensional sonic anemometer and an open path, infrared absorption gas analyzer, were placed on a scaffold tower 36.9 m above the surface (10 m above the canopy, see Table 1). The topography of this site is a challenge for flux studies. Its landscape is undulating. The vegetation around the tower changes systematically (E. M. Falge, unpublished data). As a consequence, there is a relatively large variability in flux measurements as compared with other more flat sites. At this site, diffuse PAR measurements are available through the Integrated Surface Irradiance Study (ISIS) program (http://www.atdd.noaa.gov/isis/isis.htm) [*Hicks et al.*, 1996]. Detailed information on the measurements, the site condition, and the vegetation characteristics is provided by *Wilson and Baldocchi* [2000] and *Johnson and Van Hook* [1989].

[17] The native tallgrass prairie and the winter wheat crop sites are located in north central Oklahoma, United States, in the Department of Energy (DOE) Atmospheric Radiation Measurement-Cloud and Radiation Testbed (ARM-CART) region. The former is near Shidler, and the latter is near Ponca City, both with flat terrains. The prairie, dominated by warm season C_4 grasses, is typical of the central Kansas/northern Oklahoma region. The wheat crop was planted mid October, emerged 2 weeks later, and reached maturity in late May. It was harvested early July. Fluxes of CO_2, sensible heat, latent heat, and momentum were measured at a height of 4.5 m in the center of a quarter section field (65 ha) using the EC technique. The EC array of sensors included a three-dimensional sonic anemometer, a Krypton hygrometer, and a closed-path CO_2 analyzer. Further information on methodology and measurements at the tallgrass prairie and winter wheat sites is given by *Suyker and Verma* [2001].

[18] The Scots pine forest site belongs to CarboEurope (http://www.bgc-jena.mpg.de/public/carboeur/), while the other four sites are within the network of AmeriFlux (http://cdiac.esd.ornl.gov/programs/ameriflux/). To ensure network intercomparability, AmeriFlux circulates a set of reference sensors to its members, and FLUXNET sponsors the circulation of this set of instruments to other regional networks. It has been found that intercomparability among different sites/sensors is good [*Baldocchi et al.*, 2001].

[19] This study involved one growing season of measurements from each of these five sites (Scots pine forest in 1997, aspen forest in 1996, mixed deciduous forest in 1995, and tallgrass prairie and winter wheat in 1997). The analyses were based on half-hourly measurements of NEE, air temperature, vapor pressure deficit (VPD), soil temperature, and global PAR. At each site, global PAR, air temperature, and VPD were measured above the canopy, and soil temperature was taken at the soil surface (~5 cm deep). We also needed diffuse and direct PAR information in this study. Unfortunately, measurements of diffuse and direct PAR were available only at the mixed deciduous forest site. So we used a radiation partitioning model to calculate diffuse and direct PAR for the other four sites from measured global PAR, global solar radiation, air temperature, and humidity. The model couples several well-tested relationships published in the literature and is described in Appendix A. We tested the diffuse and direct PAR calculations using measurements from the mixed deciduous forest site and found good agreement (Figure A1 in Appendix A).

3. Data Analysis Method

[20] As we pointed out in the Introduction, it is impossible to directly compare canopy photosynthesis of diffuse radiation with that of direct radiation under natural conditions. However, by inferring parameters that exclusively define canopy photosynthetic responses to diffuse and direct light from canopy CO_2 flux measurements, we can construct the canopy photosynthetic

responses to diffuse or direct light through the parameters inferred. We can then examine the differences or similarities of canopy photosynthesis of diffuse and direct light based on the constructed responses. In this section we will derive a canopy photosynthetic response function that allows us to infer parameters that exclusively define canopy photosynthetic responses to diffuse and direct light from tower flux measurements. Procedures to test the derived response function will be outlined.

3.1. A Generalized Rectangular Hyperbola

[21] For the purpose of this study, the NEE of CO_2 (F_c) measured over a plant canopy can be considered as consisting of two components: canopy photosynthetic flux density (P) and ecosystem respiration rate (R_e):

$$F_c = R_e - P. \tag{1}$$

By writing NEE in the form (1) we adopt the sign convention used by the flux community for NEE: positive upward. Ecosystem respiration (R_e) consists of carbon loss by autotrophs (roots, plants) and heterotrophs (microbes, fungi, bacteria, etc), but a gain of carbon by the atmosphere. In many empirical analyses [e.g., *Fan et al.*, 1990; *Hollinger et al.*, 1994; *Ruimy et al.*, 1995; *Hollinger et al.*, 1998; *Wofsy et al.*, 1993; *Goulden et al.*, 1997; *Chen et al.*, 1999; *Lindroth et al.*, 1998; *Lee et al.*, 1999], a rectangular hyperbola has been used to describe canopy photosynthetic flux density P:

$$\text{(Model 1)} \qquad P = \frac{\alpha I_t \beta}{\beta + \alpha I_t}, \tag{2}$$

where I_t is the global PAR incident on the canopy; α is the canopy quantum yield on an incident PAR basis when I_t approaches zero [*Wofsy et al.*, 1993], and we call it the initial canopy quantum yield; β is another empirical coefficient. Equation (2) is designated as Model 1. In previous studies, β has been explained as the maximum canopy photosynthetic flux density or canopy photosynthetic flux density at saturation because $P \to \beta$ as $I_t \to \infty$. In fact, this is not an appropriate description for this coefficient. For many crops, for example, canopy photosynthesis does not saturate at the natural range of PAR. Instead, crops show an almost linear relationship with PAR [*Ruimy et al.*, 1995]. Equation (2) itself is very flexible. Figure 1 illustrates the relationship between P and I_t for different values of β. As β increases, the curve becomes closer to being linear. At $\beta = \infty$, the curve is linear. Therefore β actually describes the closeness to linear response of the canopy photosynthetic response curves, that is, the capacity of a canopy to resist photosynthetic saturation at high levels of PAR. In other words, β is not necessarily the real canopy photosynthetic rate at saturation, and does not have to be within ranges of commonly observed canopy photosynthetic flux densities. For semantic clearness, β will be referred to as Closeness to Linear Response (CLR) coefficient thereafter.

[22] Previous studies have always treated α and β as purely canopy properties and fixed them for a given plant canopy under study. Such a view needs to be changed. Because of the differential responses of canopy photosynthesis to diffuse and direct PAR, as pointed out in the Introduction, these two parameters likely depend on sky conditions as well. *Norman and Arkebauer* [1991] and *Choudhury* [2000, 2001a, 2001b] showed that modeled LUE at the canopy level increases linearly with the diffuse fraction. To represent this modeling finding, *Anderson et al.* [2000] described canopy LUE by the product of the nominal LUE and a linear function of diffuse fraction with the nominal LUE equal to canopy LUE when the diffuse faction is 0.5. In this study, we generalize the results of these researchers and assume that both α and β are linear functions of the fractions of diffuse and direct light in global PAR. Thus

$$\alpha = \alpha_f \frac{I_f}{I_t} + \alpha_r \frac{I_r}{I_t}, \tag{3}$$

$$\beta = \beta_f \frac{I_f}{I_t} + \beta_r \frac{I_r}{I_t}, \tag{4}$$

where α_f and α_r are the initial canopy quantum yield for diffuse (I_f) and direct (I_r) PAR, respectively, and β_f and β_r are the CLR coefficient for diffuse and direct PAR, respectively. Our treatment of α (equation (3)) is similar to the treatment of LUE by *Anderson et al.* [2000] in the sense that both are linear functions of the diffuse fraction. To our knowledge, the introduction of (4) is new in this paper. Substituting (3) and (4) into (2), we have

$$\text{(Model 2)} \qquad P = \frac{(\alpha_f I_f + \alpha_r I_r)(\beta_f I_f + \beta_r I_r)}{(\beta_f I_f + \beta_r I_r) + (\alpha_f I_f + \alpha_r I_r) I_t}. \tag{5}$$

Equation (5), which is designated as Model 2, can be considered as a generalization to the commonly used rectangular hyperbola (Model 1, equation (2)). At the extreme condition when the canopy receives only purely diffuse (direct) radiation, $I_r = 0$ ($I_f = 0$), equation (5) reduces to the exact form of equation (2). If there are no differences between diffuse and direct PAR for canopy photosynthesis, $\alpha_r = \alpha_f$ and $\beta_r = \beta_f$, equation (5) also returns to equation (2). Therefore α_f (α_r) and β_f (β_r) in equation (5) have the same meanings with α and β, respectively, in equation (2). They describe the characteristics of canopy photosynthetic responses to diffuse and direct PAR, respectively. Later we will examine the differences in canopy photosynthetic efficiencies between diffuse and direct PAR by comparing α_r with α_f and β_r with β_f. Higher values of α_r (α_f) or β_r (β_f) indicate better efficiencies.

[23] The dependence of ecosystem respiration rate R_e is described by the following function:

$$R_e = c_1 e^{c_2[c_3 T_a + (1-c_3)T_s]} + d_1 e^{d_2 T_s}, \tag{6}$$

where c_1, c_2, c_3, d_1, and d_2 are regression coefficients, T_s is soil temperature, and T_a is air temperature. The first term on the right-hand side of equation (6) is expected to capture aboveground biomass respiration, while the second is expected to capture soil respiration. Instead of using only air temperature in the first term on the right-hand side of (6), we employ $c_3 T_a + (1 - c_3)T_s$ to reflect the effects of vertical temperature gradient on aboveground biomass respiration. Obviously, $0 \le c_3 \le 1$.

3.2. Statistical Model Testing Procedures

[24] Two questions need to be answered in the model testing: (1) Does the generalized rectangular hyperbola (Model 2, equation (5)), which treats diffuse and direct PAR explicitly, work effectively for a wide range of vegetation types? (2) By including diffuse and direct PAR information in the model, do we improve model performance?

[25] To answer these questions, we divided the growing seasons of the five sites into 11-day moving windows (see the following section). For each window we randomly separated the measurements into two parts: one part for estimating coefficients through nonlinear regression procedures (regression data set), and the other for independently validating models (validation data set). We used both the measured and calculated diffuse and direct PAR in the test of Model 2 for the mixed deciduous forest site.

[26] To examine the importance of separating diffuse and direct PAR in predicting canopy photosynthesis, we compare the new model with the conventional rectangular hyperbola (Model 1),

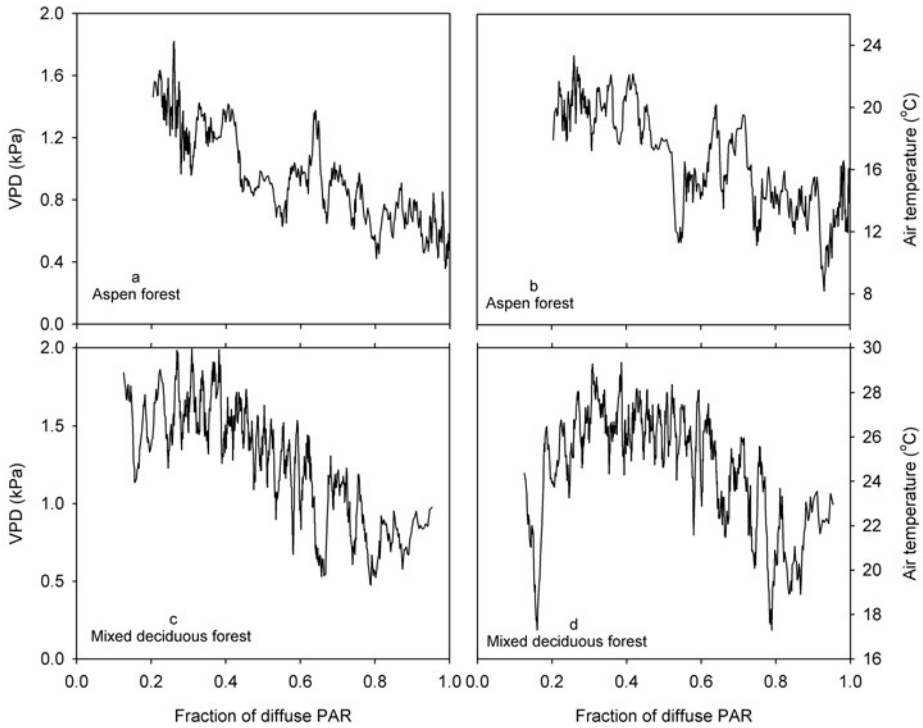

Figure 2. Changes of VPD and air temperature with the ratio of diffuse to global PAR at (a and b) the aspen forest site (calculated diffuse PAR, solar elevation 50°–60°) and (c and d) the mixed deciduous forest site (measured diffuse PAR, solar elevation 60°–70°). Data were moving-averaged with 11 points. In the moving average the ordering was done on the fraction of diffuse PAR, and the averaging was done on VPD and air temperature.

which assumes the same canopy photosynthetic effects for diffuse and direct PAR (photosynthetic parameters are therefore treated as constants for a given canopy).

[27] For reasons explained later, we do not intend to introduce effects of temperature (except on ecosystem respiration) and VPD explicitly into Model 2. To examine how critical the roles of temperature and VPD are in the regression scheme, we compared Model 2 with a multiple response function that is similar to those used by global GPP models [e.g., *Reed et al.*, 1976; *Prince*, 1991; *Law and Waring*, 1994; *Runyon et al.*, 1994; *Landsberg et al.*, 1995; *Prince and Goward*, 1995]. The multiple response function has the following form:

$$\text{(Model 3)} \qquad P = \frac{\alpha I_t \beta}{\beta + \alpha I_t} f(T_a) f(V), \tag{7}$$

where V is VPD. The parameters $f(T_a)$ and $f(V)$ are environmental response functions to modulate canopy photosynthetic responses to light given by

$$f(T_a) = \frac{\exp\left(\frac{a_1(T_a - T_r)}{RT_rT_a}\right)}{1 + \exp\left(\frac{a_2(T_a - T_m)}{RT_rT_a}\right)}$$
$$f(V) = \frac{1}{1 + b_1 \exp(-b_2/V)}, \tag{8}$$

where a_1, a_2, T_m, b_1, and b_2 are coefficients to be estimated through regression, T_r is the reference temperature (25°C), and R is the gas constant. The term $f(T_a)$ has been widely used to describe leaf physiological response to changes in temperature [*Harley and Tenhunen*, 1991]. The VPD response function has a feature of being equal to unity when the air is saturated (V = 0) and decreasing when VPD increases. The design of $f(V)$ reflects considerations of results published in the literature concerning responses of plant physiological activities to VPD [*Runyon et al.*, 1994; *Law and Waring*, 1994; *Hogg et al.*, 2000].

[28] Following the recommendations of *Willmott* [1981, 1982], we employed three statistical indices together in the model testing and comparisons in order to give adequate evaluation on the overall performance of these models. The three indices are r^2, root-mean-square error (RMSE), and index of agreement (IOA) [*Willmott*, 1981, 1982]. IOA has the advantage of being both differential (as opposed to r^2) and bounded (no agreement 0 $\leq$ IOA $\leq$ 1 complete agreement, as opposed to RMSE) and therefore complements r^2 and RMSE. For each moving window, values of r^2, RMSE, and IOA were calculated for each of the three models and for both regression and validation data sets. The paired t test was then conducted to evaluate the significance regarding the differences in r^2, RMSE, and IOA between Model 2 and Model 1 and Model 3 for both model regression and validation.

3.3. Obtaining Seasonal Dynamics

[29] After the new model (Model 2) was tested, the measurements were merged. To get the seasonal dynamics of the initial canopy quantum yield and CLR coefficient for both diffuse PAR (α_f and β_f) and direct PAR (α_r and β_r), we applied an 11-day moving window technique. The obtained values from a given 11-day window were treated as the values for the central day of the window (5 days before and after the central day). The length of this 11-day window is a trade-off between two competing requirements. The first requirement is that it must be short enough so that no significant changes in canopy structure and leaf physiology

Table 2. Statistics of the Paired *t* Tests on the Differences Between Model 2 and Model 1, Model 2 and Model 3 in the r^2 for Model Regression (Reg.) and Validation (Val.)

	Mixed[a]	Mixed[b]	Aspen	Scots Pine	Prairie	Wheat
Model 2 – Model 1						
Reg.						
t stat	11.70	9.67	21.15	20.12	13.96	4.07
$t_{0.05}$	1.65	1.65	1.66	1.66	1.66	1.66
P value	0.00	0.00	0.00	0.00	0.00	0.00
Val.						
t stat	12.45	8.46	17.20	9.44	12.28	5.43
$t_{0.05}$	1.65	1.65	1.66	1.66	1.66	1.66
P value	0.00	0.00	0.00	0.00	0.00	0.00
Model 2 – Model 3						
Reg.						
t stat	1.42	−2.15	13.28	10.34	5.84	−1.10
$t_{0.05}$	1.65	1.65	1.66	1.66	1.66	1.66
P value	0.08	0.80	0.00	0.00	0.00	0.86
Val.						
t stat	5.05	1.41	12.85	7.16	7.92	1.88
$t_{0.05}$	1.65	1.65	1.66	1.66	1.66	1.66
P value	0.00	0.08	0.00	0.00	0.00	0.03

[a] Using measured diffuse/direct PAR.
[b] Using calculated diffuse/direct PAR.

occur during this period. The second requirement is that it must be long enough to have sufficient data points for regressional analyses. The length scale of 11 days also covers frontal passages that often cause large flux spectral variance [*Baldocchi and Wilson*, 2001]. This coverage is important for this study since it widens the range of sky conditions and therefore the ranges of diffuse and direct PAR in the moving window and increases the stability and reliability in the estimates of photosynthetic parameters through nonlinear regressions. The seasonal courses were obtained by moving the window day by day.

[30] We examined how errors in the calculated diffuse and direct PAR affect the estimates of α_f, β_f, α_r, and β_r. We determined the seasonal patterns of α_f, β_f, α_r, and β_r using both measured and calculated diffuse and direct PAR for the mixed deciduous forest site. A sensitivity analysis was conducted to see how the estimates of the parameters change in responses to ±15% variation in the calculated diffuse PAR (direct PAR varied accordingly so that global PAR is unchanged).

3.4. Nonlinear Regression

[31] A nonlinear regression software package called ODRPACK was used in this study. ODRPACK can be freely downloaded from http://www.netlib.org/. Although the major feature of this software is its weighted orthogonal distance regression, we chose to use its ordinary least squares function after numerous trials. This is because in our regression the measurement errors of the dependent variable (NEE) are much greater than the measurement errors of explanatory variables (direct PAR, diffuse PAR, air temperature, VPD, etc.). To invoke the weighted orthogonal distance regression, one must be very careful in selecting the delicate weights for both dependent and explanatory variables, which is very difficult to do. In the end, we concluded that the weighted orthogonal distance

Table 3. Statistics of the Paired *t* Tests on the Differences Between Model 2 and Model 1, Model 2 and Model 3 in the Root-Mean-Square Error (RMSE) for Model Regression (Reg.) and Validation (Val.)[a]

	Mixed[b]	Mixed[c]	Aspen	Scots Pine	Prairie	Wheat
Model 2 – Model 1						
Reg.						
t stat	−11.78	−10.56	−21.27	−19.95	−15.64	−6.32
$t_{0.05}$	−1.65	−1.65	−1.66	−1.66	−1.66	−1.66
P value	0.00	0.00	0.00	0.00	0.00	0.00
Val.						
t stat	−13.70	−7.96	−19.37	−9.43	−14.87	−8.41
$t_{0.05}$	−1.65	−1.65	−1.66	−1.66	−1.66	−1.66
P value	0.00	0.00	0.00	0.00	0.00	0.00
Model 2 – Model 3						
Reg.						
t stat	−2.16	1.24	−12.21	−11.54	−7.63	−2.59
$t_{0.05}$	−1.65	−1.65	−1.66	−1.66	−1.66	−1.66
P value	0.02	0.89	0.00	0.00	0.00	0.006
Val.						
t stat	−3.61	−3.92	−15.62	−8.15	−9.83	−5.37
$t_{0.05}$	−1.65	−1.65	−1.66	−1.66	−1.66	−1.66
P value	0.00	0.00	0.00	0.00	0.00	0.00

[a] RMSE is in units of μmol m^{-2} s^{-1}.
[b] Using measured diffuse/direct PAR.
[c] Using calculated diffuse/direct PAR.

Table 4. Statistics of the Paired *t* Tests on the Differences Between Model 2 and Model 1, Model 2 and Model 3 in the Index of Agreement for Model Regression (Reg.) and Validation (Val.)

	Mixed[a]	Mixed[b]	Aspen	Scots Pine	Prairie	Wheat
Model 2 – Model 1						
Reg.						
t stat	12.40	9.79	22.49	15.90	15.84	6.23
$t_{0.05}$	1.65	1.65	1.66	1.66	1.66	1.66
P value	0.00	0.00	0.00	0.00	0.00	0.00
Val.						
t stat	12.06	8.83	18.71	5.44	14.76	5.96
$t_{0.05}$	1.65	1.65	1.66	1.66	1.66	1.66
P value	0.00	0.00	0.00	0.00	0.00	0.00
Model 2 – Model 3						
Reg.						
t stat	0.54	2.04	12.60	11.70	5.51	0.46
$t_{0.05}$	1.65	1.65	1.66	1.66	1.66	1.66
P value	0.29	0.98	0.00	0.00	0.00	0.32
Val.						
t stat	4.42	0.33	13.17	7.85	8.57	4.08
$t_{0.05}$	1.65	1.65	1.66	1.66	1.66	1.66
P value	0.00	0.63	0.00	0.00	0.00	0.00

[a] Using measured diffuse/direct PAR.
[b] Using calculated diffuse/direct PAR.

regression does not necessarily provide better estimations of parameters than the ordinary least squares regression in our case and the ordinary least squares regression (no weights applied to data points) is sufficient for our analyses.

[32] The regression was conducted for each window. In the nonlinear regressions it is necessary to pick up a set of initial guesses for the parameters that are to be estimated. Sometimes the nonlinear regression cannot end with the desired sum of squares convergence with one trial of initial guesses. To deal with this problem, we employed a repetitive regression procedure. If the regression fails to converge, the procedure goes back and reinitializes the regression with a different set of initial guesses. The initial guesses are picked up randomly from the preset reasonable ranges (based on previous knowledge). The process repeats until the proper convergence is reached, or until the maximum of 50 cycles is reached. If the latter case happens, the current window is abandoned, and the regression moves to the next window.

3.5. Some Additional Points About the Generalized Rectangular Hyperbola

[33] It is important to point out that the initial canopy quantum yield of direct PAR (α_r) is not equivalent to the initial canopy quantum yield for clear days. Under clear skies the fraction of diffuse radiation changes with solar elevation angles. This fraction approaches unity when solar elevation is less than 5° but decreases as solar elevation increases [*Goudriaan*, 1977]. The initial canopy quantum yield is determined from the initial response of canopy photosynthesis to PAR when PAR is low. Under clear skies, low levels of global PAR can only occur in early morning and late afternoon when the Sun is near the horizon. Since a high fraction of global PAR at the Earth surface is diffuse under these solar positions, the initial slopes of the curves of canopy photosynthesis against global PAR obtained from clear days would typically have a diffuse "signature." Therefore the light response curves obtained separately from clear and cloudy days should converge at the low light level, and they both should be close to the slope of purely diffuse PAR (α_f).

[34] In theory, both α_r and β_r should depend on solar elevation angles since the fraction of sunlit leaves in canopies changes with the direct beam incidental angle. However, our analyses using models of *Ross* [1981] showed that the fraction of sunlit leaves is sensitive to changes in solar elevation angles only when the Sun is near the horizon. As the solar elevation increases, the fraction of sunlit leaves increases but quickly saturates and is not sensitive to changes in solar elevation angles at high solar positions. Under natural conditions, direct beam radiation dominates only at high solar elevation angles. Therefore we expect that the dependence of α_r and β_r on solar elevation angles is small.

[35] Diffuse and direct PAR, temperature, and VPD are correlated with each other under natural conditions (Figure 2). Because of this correlation, applying additional temperature and VPD response functions to Model 2 may result in multicollinearity [*Ratkowsky*, 1989; *Myers*, 1990] and confound the estimates of initial canopy quantum yield and CLR coefficient through nonlinear regression. This is not desirable because we are not only interested in the overall performance of Model 2 but also want to make sure that its parameters have clear biophysical meanings. Therefore it serves the particular goal of this paper by keeping regressors simple and independent in Model 2.

[36] Since Model 2 does not explicitly consider the effects of temperature and VPD on canopy photosynthesis, they must be reflected through the parameters of α_f, α_r, β_f, and β_r. A question arises naturally: Are the differences between α_f and α_r, β_f and β_r attributable to the differences in the canopy photosynthetic effects of diffuse and direct PAR? The answer is yes. Note that values of α_f, α_r, β_f, and β_r are determined at the same time domain for diffuse and direct PAR through Model 2. If at a certain time of the growing season, a certain environmental condition (e.g., water stress or no water stress) affects the photosynthesis of direct PAR, this same condition affects the photosynthesis of diffuse PAR also. What interests us are the relative magnitudes of α_f against α_r, β_f against β_r. Therefore the dependence of α_f, α_r, β_f, and β_r on temperature, VPD, or any other environmental conditions does not pose any problem to our analyses as long as they are always compared with each other under the same environmental conditions.

[37] It should be clear that the differences between α_f and α_r, β_f and β_r as estimated from Model 2 are not the same as the differences between cloudy and clear days in α and β as estimated from Model 1. As we explained in the Introduction and also in the work of *Gu et al.* [1999], many environmental factors can differ between cloudy and clear days. It would be difficult to identify environmental factors that are responsible for the differences in α and β of Model 1 between cloudy and clear

Table 5. Average Diffuse and Direct Canopy Photosynthetic Parameters and Their Standard Errors[a]

	Mixed[b]	Mixed[c]	Aspen	Scots Pine	Prairie	Wheat
Mean α_f	4.93 ± 0.14	4.34 ± 0.14	2.90 ± 0.05	2.89 ± 0.06	2.19 ± 0.07	2.08 ± 0.14
Mean α_r	2.33 ± 0.09	2.43 ± 0.12	1.35 ± 0.04	1.83 ± 0.06	1.62 ± 0.06	1.58 ± 0.13
Mean α_f / α_r ratio	2.81 ± 0.17	3.49 ± 0.53	2.50 ± 0.21	1.67 ± 0.04	1.41 ± 0.03	1.66 ± 0.08
Mean β_f	69.7 ± 5.6	63.8 ± 5.4	239.2 ± 17.2	80.0 ± 5.3	238.0 ± 9.6	95.3 ± 6.3
Mean β_r	20.4 ± 0.84	22.7 ± 1.1	25.8 ± 2.3	20.0 ± 0.7	20.1 ± 1.1	24.0 ± 2.5
Mean β_f and β_r ratio	4.7 ± 0.7	3.6 ± 0.3	15.4 ± 1.5	6.3 ± 0.8	13.9 ± 0.5	8.2 ± 0.7

[a] Averaging periods are the same as in Figures 5 and 8. Units of initial canopy quantum yields α_f and α_r are in 100 × mol CO_2/mol photon; CLR coefficients β_f and β_r are in μmol m^{-2} s^{-1}.
[b] Using measured diffuse/direct PAR.
[c] Using calculated diffuse/direct PAR.

days. This is why we used Model 2 and did not group days for cloud types in this study.

4. Results

4.1. Model Test and Comparisons

[38] Results of the paired *t* tests on the differences in all three statistics (r^2, RMSE, and index of agreement) between Model 2 and Model 1 indicate that Model 2, which has higher r^2 and index of agreement and smaller RMSE, consistently performs better than Model 1 with statistical significance for all five sites and for both regression and validation (see Table 2 for r^2, Table 3 for RMSE, and Table 4 for index of agreement). In all these tests the *P* values are smaller than 0.0001.

[39] For the comparisons between Model 2 and Model 3 the statistical test results are mixed. For the sites of aspen forest, Scots pine forest, and tallgrass prairie, results of the paired *t* tests on the differences in all three statistics between Model 2 and Model 3 show that Model 2 consistently performs better than Model 3 with statistical significance for both regression and validation (see Tables 2, 3, and 4). In these tests the *P* values are also smaller than 0.0001. For the winter wheat site the validation tests on all three statistics indicate that Model 2 works better than Model 3. The regression test on RMSE also supports this statement. However, the regression tests on r^2 and index of agreement indicate that there are no significant differences between Model 2 and Model 3. For the mixed deciduous forest site, both measured and calculated diffuse and direct PAR were used in the model comparisons. For this site the following paired *t* tests suggest that Model 2 is better: r^2 with validation data set and measured diffuse and direct PAR, RMSE with regression data set and measured diffuse and direct PAR, RMSE with validation data set and both measured and calculated diffuse and direct PAR, index of agreement with validation data set and measured diffuse and direct PAR. However, other tests at this site indicate no significant differences between Model 2 and Model 3. The mixed results in the statistical tests of r^2, RMSE, and index of agreement suggest that the recommendations made by *Willmott* [1981, 1982] on model evaluations are probably valid.

[40] Although we expect that Model 2 is better than Model 1, the better performance of Model 2 than Model 3 for most cases tested is somewhat surprising since Model 3 has more driving variables and free regression coefficients than Model 2. These results indicate that it is important to separate diffuse and direct PAR in interpreting NEE measurements. For some ecosystems the importance of doing so may even exceed the inclusion of temperature and VPD in the predicting schemes of NEE. The reason for that is diffuse radiation is correlated with VDP and temperature and represents a combined measure of both effects (Figure 2).

[41] By comparing the *t* statistics and *P* values for the tests of using measured diffuse and direct PAR and those of using calculated diffuse and direct PAR for the mixed deciduous forest site, one finds that using measured diffuse and direct PAR increases the differences between Model 2 and Model 1 as well as the differences between Model 2 and Model 3 (see Tables 2, 3, and 4).

[42] The effectiveness of the generalized rectangular hyperbola (Model 2) in predicting NEE can also be examined in Figures 3 and 4 for model fitting and independent model validation, respectively. In general, the calculated NEE closely agrees with the measured NEE. The values of r^2, RMSE, and index of agreement indicate that the generalized rectangular hyperbola works well for the five sites. The values of the three statistical indices vary from site to site, which reflects variations in site complexity. The mixed deciduous forest site, which is the most complex site, has the lowest values of r^2 and index of agreement and largest RMSE among the five sites studied. The model tends to underestimate the magnitude of unusually large fluxes (positive or negative). This is probably not caused by the model. For example, ecosystem respiration rates, which are shown to exceed 10 μmol m^{-2} s^{-1} in some measurements, are hard to explain ecologically for these northern sites. It is known that occasionally the eddy covariance technique obtains unusually large fluxes (either positive or negative). However, these points are sporadic and more likely due to certain atmospheric turbulent events than to any real ecological or physiological processes.

4.2. Advantages of Diffuse PAR: Initial Canopy Quantum Yields α_f and α_r

[43] All five sites show that the initial canopy quantum yield of diffuse PAR (α_f) is consistently higher than the initial canopy quantum yield of direct PAR (α_r) (Figure 5). For the mixed deciduous forest in Oak Ridge, Tennessee, the seasonal patterns using measured diffuse and direct PAR (Figure 5a) are similar to those using calculated diffuse and direct PAR (Figure 5b) although sometimes using calculated diffuse and direct PAR leads to smaller estimates for α_f and larger estimates for α_r (for example, compare values of α_f and α_r around day 200 in Figures 5a and 5b). Again, vegetation and land complexities and perhaps variable weather conditions at this mixed deciduous forest site lead to large day-to-day variations in the estimates of α_f and α_r, while at other sites (Figures 5c–5f) changes are smoother. Seasonality of α_f and α_r can be clearly seen at the tallgrass prairie site (Figure 5e) and the winter wheat site (Figure 5f). At the tallgrass prairie site, both α_f and α_r increase during the spring period and reach the maximum in the midsummer and then decrease toward the end of the growing season (Figure 5e). Several developmental stages in the growth of winter wheat are revealed by the temporal patterns of α_f and α_r (Figure 5f). In early growth stages of winter wheat, α_f and α_r, which are both small, do not differ very much. As the wheat develops, both α_f and α_r increase as well as the differences between them. However, as it approaches maturity, the two parameters converge again and then decrease rapidly toward the end of May (Figure 5f). The seasonality of α_f and α_r at the Scots pine forest site (Figure 5c) and the aspen forest site (Figure 5d) is not as clear as at the tallgrass prairie site or the winter wheat site although increases during spring and decreases during autumn can still be seen at the two sites.

[44] The sensitivity test shows that ±15% variations in the calculated diffuse PAR and accordingly in the calculated direct PAR have hardly any effects on the estimates of α_r and only

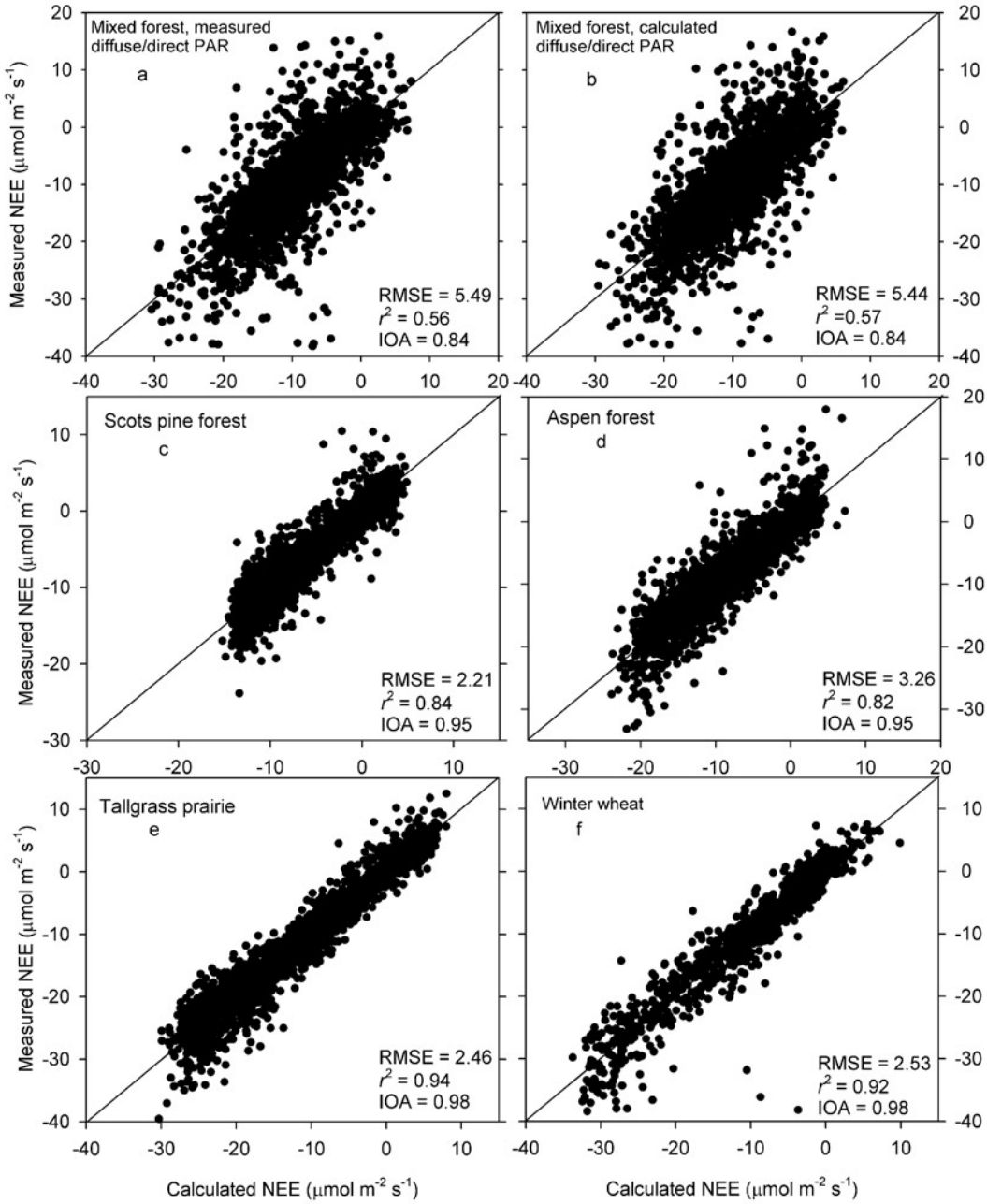

Figure 3. Agreement between the Model 2 calculated and measured NEE for the mixed deciduous forest using (a) measured diffuse and direct PAR and (b) calculated diffuse and direct PAR, (c) Scots pine forest, (d) aspen forest, (e) tallgrass prairie, and (f) winter wheat for model fitting.

slightly affect the estimates of α_f. For clearness, we show the ±15% test curves only for the aspen site in Figure 5. A +15% change in the calculated diffuse PAR slightly reduces the estimates of α_f, and a −15% change slightly increases the estimates of α_f, while the effects on α_r are hardly detectable (Figure 5d). Together with the results from the mixed deciduous forest site where both measured and calculated diffuse and direct PAR are used, we therefore conclude that errors in the calculated diffuse and direct PAR are unlikely responsible for the differences between α_f and α_r obtained here.

[45] The ratios of α_f to α_r at the five sites are compared in Figure 6. Although there are a lot of scatterings in the data points, the α_f to α_r ratio is generally greater than 1. The mean values of α_f, α_r, and the α_f to α_r ratio at the five sites are found in Table 5. The mixed deciduous forest has the largest mean α_f (0.049 and 0.043 mol CO_2/mol photon using measured and calculated diffuse and direct PAR, respectively) and α_r (0.023 and 0.024 mol CO_2/mol photon using measured and calculated diffuse and direct PAR, respectively). The winter wheat has the smallest mean α_f (0.021 mol CO_2/mol photon), while the aspen

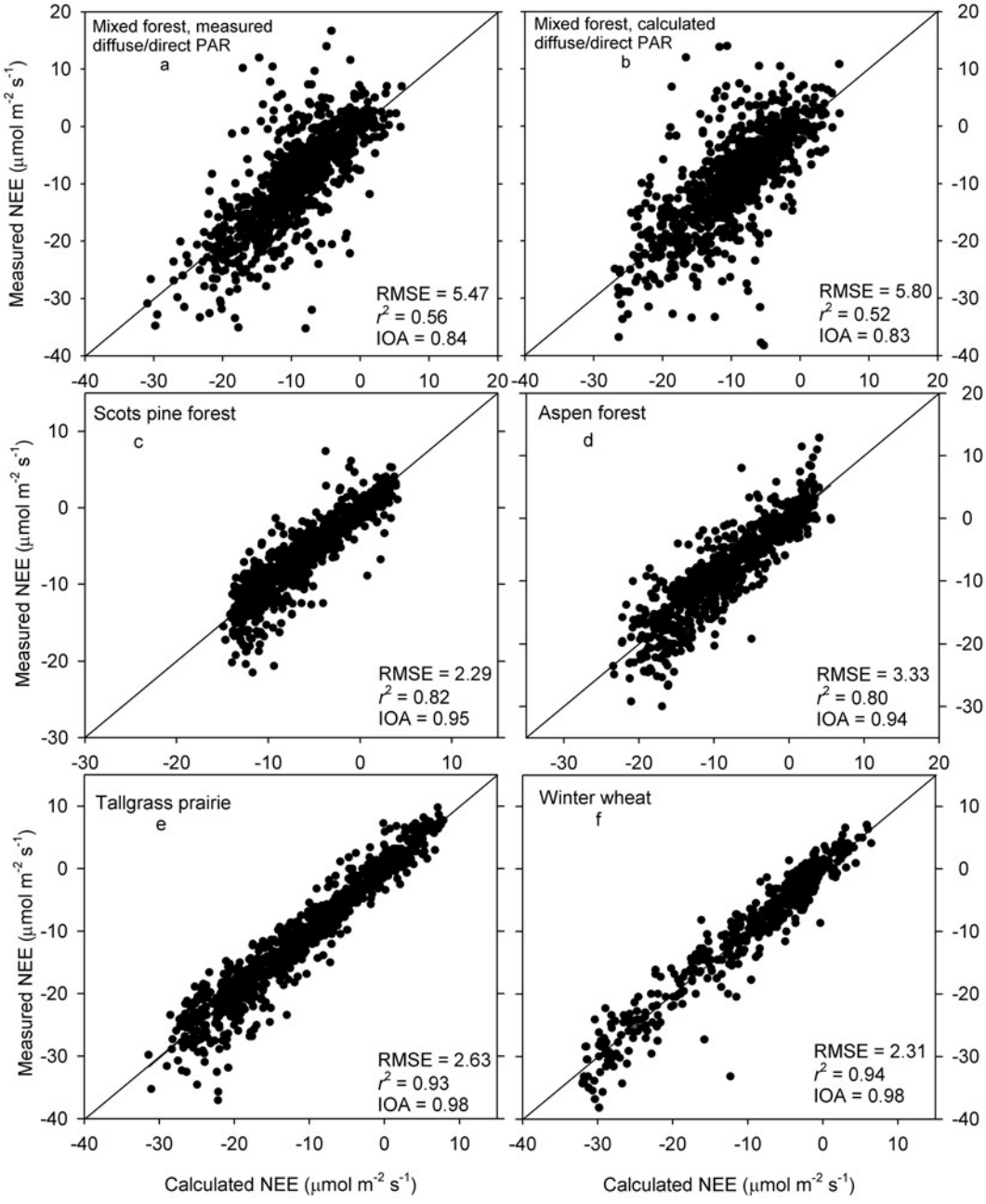

Figure 4. Same as Figure 3, but for model validation.

forest has the least mean α_r (0.014 mol CO_2/mol photon). The mixed deciduous forest also has the largest mean α_f to α_r ratio (2.81 and 3.49 using measured and calculated diffuse and direct PAR, respectively), while the tallgrass prairie has the least mean α_f to α_r ratio. Because of the strong seasonality in α_f and α_r at the tallgrass prairie and winter wheat sites, these mean values are for references only.

4.3. Effects of Temperature and VPD on Initial Canopy Quantum Yields α_f and α_r

[46] As we pointed out earlier, effects of temperature and VPD on canopy photosynthesis are implicitly expressed in the values of the parameters in Model 2. From Figure 5 we see that both α_f and α_r vary a lot over the season. Although the overall seasonal patterns may be controlled by leaf phenology, short-term variations are likely caused by changes in weather conditions.

[47] Since α_f and α_r are estimated through 11-day moving windows, it is not possible to conduct a strict analysis on how environmental factors control them. However, if we focus on the general patterns and prominent features only and refrain from interpreting details, we may still be able to get some insights on this issue by examining how α_f and α_r change with daily mean values of air temperature and VPD. An initial examination on Figure 5 encourages this effort. For example, a sharp drop in α_f and a somewhat less significant drop in α_r occurred early in the growing season, around day 172, in the aspen forest (Figure 5d). The temporal records of surface meteorological variables indicated that this was associated with the passage of a cold front. During

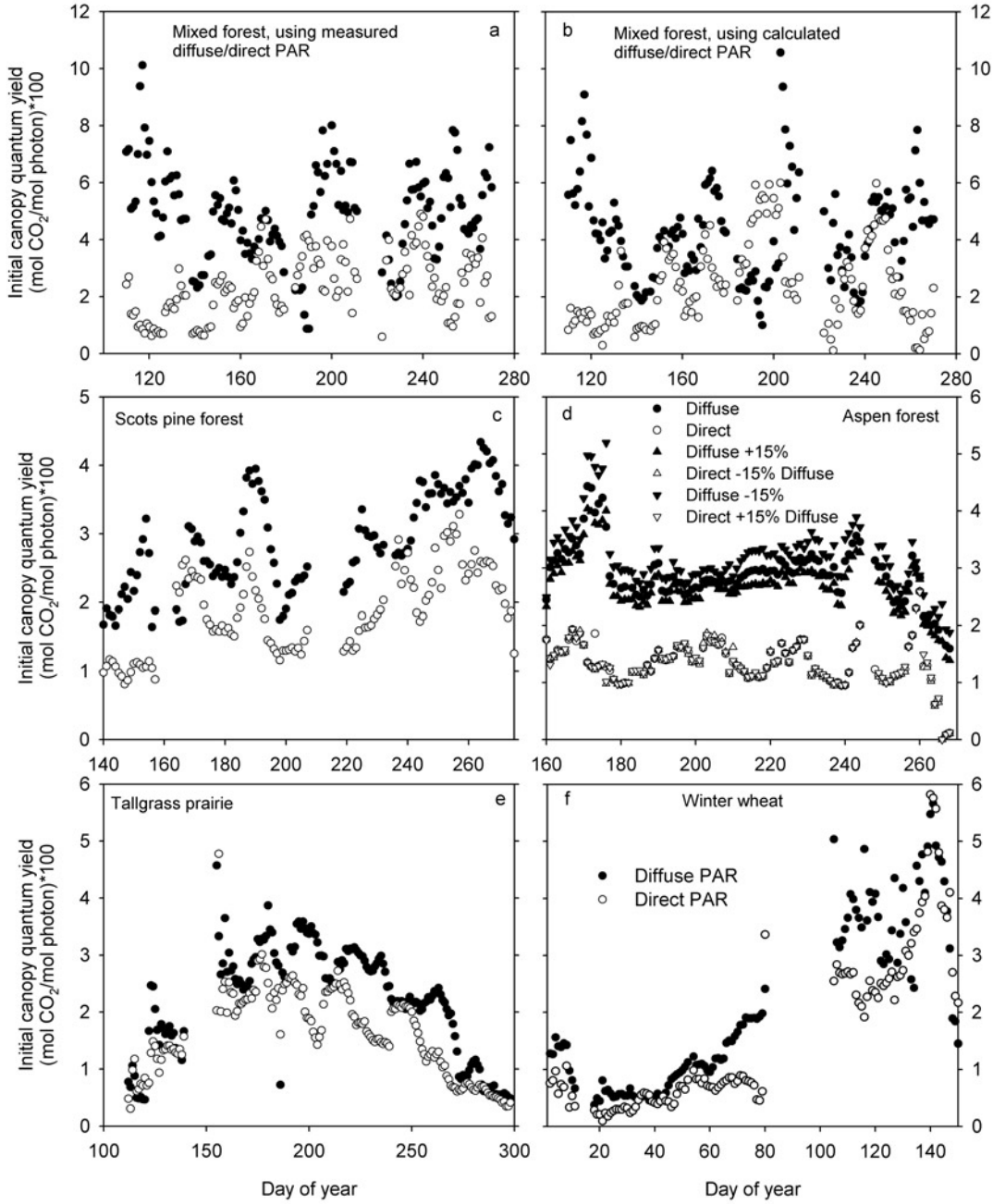

Figure 5. Seasonal dynamics of diffuse and direct initial canopy quantum yields α_f and α_r for the mixed deciduous forest using (a) measured diffuse and direct PAR and (b) calculated diffuse and direct PAR, (c) Scots pine forest, (d) aspen forest, (e) tallgrass prairie, and (f) winter wheat. The sensitivity test results are shown for the aspen forest (Figure 5d). In the sensitivity test the diffuse PAR is varied by ±15% over the calculated values, and the direct PAR is varied accordingly to keep the measured global PAR unchanged. The obtained seasonal patterns are shown along with the original calculations. For clarity, sensitivity test results for other sites are not shown. Most missing points are due to gaps in the original measurements. A few are due to unsuccessful convergence in the regression.

this period, surface air pressure increased, and the wind direction shifted from steady southwesterly to northwesterly wind. In the meantime, mean daily air temperature dropped 12°C in less than 3 days and reached a minimum of less than 4°C. We noticed that the highest α_f before this event was about 0.046 mol CO_2/mol photon. Such a high value was never reached again after the cold weather front was past (Figure 5d). In the following, we will analyze changes of α_f and α_r with air temperature and VPD using data from the mid growing seasons at the five sites (days 150–275 for the Scots pine forest, 160–270 for the aspen forest, 110–270 for the mixed deciduous forest, 160–260 for the tallgrass prairie, 110–150 for the winter wheat) to minimize the impact of phenology.

[48] Among the five sites, Scots pine forest appears to be most sensitive to changes in air temperature (Figure 7a). However, the

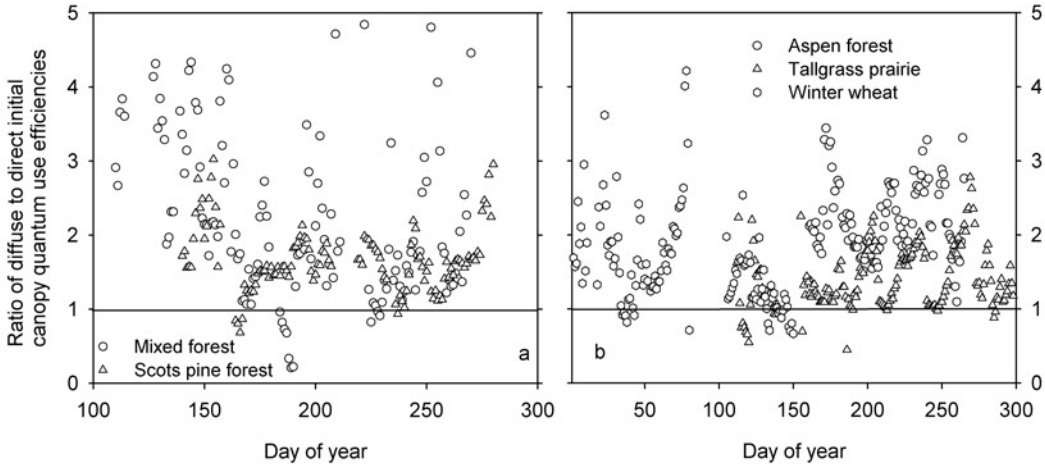

Figure 6. Ratios of diffuse to direct initial canopy quantum yields α_f/α_r for the (a) mixed deciduous forest (using measured diffuse and direct PAR) and Scots pine forest and (b) aspen forest, tallgrass prairie, and winter wheat.

optimum temperatures for α_f and α_r, which are about 10°C, are surprisingly low. The α_f and α_r of the aspen forest respond weakly to changes in temperature (Figure 7c). Nevertheless, it can still be seen from the exhibited patterns that low or high temperatures tend to reduce α_f and α_r. The optimum temperatures for α_f and α_r appear to be around 15°C. The α_f and α_r of the mixed deciduous forest (Figure 7e) respond to temperature differently at low temperature range. While α_f is higher for temperature <20°C than for temperature >20°C, the opposite is true for α_r. No clear dependence of α_f and α_r of the tallgrass prairie on temperature is identifiable (Figure 7g). Similar to the mixed deciduous forest (Figure 7e), the α_f and α_r of winter wheat (Figure 7i) also respond differently to temperature. While the dependence of α_f on temperature is weak, the α_r strongly depends on temperature.

[49] The responses of α_f and α_r to VPD unavoidably carry some similarities with the responses to temperature since the two variables are correlated. For example, the initial increases in α_f and α_r of the Scots pine forest (Figure 7b) and the aspen forest (Figure 7d) with VPD are probably a reflection of the corresponding temperature responses in Figures 7a and 7c, respectively. However, the mixed deciduous forest (Figures 7e and 7f) and the tallgrass prairie (Figures 7g and 7h) show signs of independent VPD and temperature effects. In the case of the mixed deciduous forest, no clear signs of VPD effects on α_f and α_r are visible at low VPD (Figure 7f), while low temperature affects α_f and α_r (Figure 7e). Although the α_f and α_r of the tallgrass prairie apparently do not depend on temperature (Figure 7g), high VPD tends to decrease them (Figure 7h).

[50] The revelation that α_f and α_r sometimes respond to temperature as well as VPD in different ways is interesting. It explains some contrasting features between α_f and α_r in Figure 5. Although α_f and α_r show some degree of parallel changes with time in their seasonal dynamics, especially for the overall patterns, out-of-phase fluctuations in the two parameters do occur. This may indicate that environmental controls on α_f and α_r can differ.

4.4. Advantages of Diffuse PAR: CLR Coefficients β_f and β_r

[51] The relative effectiveness of diffuse and direct PAR for canopy photosynthesis can also be examined through β_f and β_r with greater values indicating lower tendency to saturation under high levels of light (see equation (4) and Figure 1). Advantages of diffuse PAR over direct PAR for canopy photosynthesis are again demonstrated by the much larger β_f than β_r for all five sites studied (Figure 8). For these sites, direct PAR more easily causes canopy photosynthetic saturation than diffuse PAR. Because β_f can be several orders of magnitude larger than β_r, the logarithmic scale is used in Figure 8. All five sites show strong seasonality in the estimates of β_f and β_r. This is in contrast with α_f and α_r, which exhibit clear seasonality only at the tallgrass prairie and winter wheat sites. The five sites have distinctively different features in the seasonal patterns of β_f and β_r. At the mixed deciduous forest site (Figure 8a, using measured diffuse and direct PAR; Figure 8b, using calculated diffuse and direct PAR), β_f and β_r increase quickly during the springtime, reach the maximum around mid May, and then gradually decrease. The maximal β_f seems to be around late July or early August for the Scots pine forest (Figure 8c), while the pattern is not clear for β_r. The seasonal patterns of β_f and β_r of the aspen forest (Figure 8d) appear to be similar to those of the mixed deciduous forest (Figures 8a or 8b), but the changes with time are gentler in the former. At the tallgrass prairie site the seasonal patterns of β_f and β_r (Figure 8e) are in contrast with those of α_f and α_r (Figure 5e). While α_f and α_r of the tallgrass prairie keep changing in the mid growing season, there is a quite long period in which β_f and β_r are relatively constant. β_f and β_r of the winter wheat increase as it approaches maturity (Figure 8f). Just like α_f and α_r (Figure 5f), β_f and β_r of the winter wheat also converge and then decrease when maturity is reached.

[52] The revealed seasonal patterns of β_f and β_r indicate that canopy photosynthesis may shift between nonlinear and linear responses to PAR during the growing period. The general trend of transition from nonlinear response early in the growing season to more linear response in the middle of growing season and then back to nonlinear response late in the growing season may reflect temporal changes in a variety of biotic factors. *Baldocchi and Amthor* [2001] used a model to show that canopy photosynthetic light responses are nonlinear at low LAI but become more linear at high LAI. The seasonal dynamics in leaf nitrogen content may also affect the seasonal patterns of β_f and β_r. The maximum catalytic activity of Rubisco (V_{cmax}) increases with leaf nitrogen content [*Wilson et al.*, 2000], while β_f and β_r should increase with V_{cmax}.

[53] Using the measured and calculated diffuse and direct PAR lead to similar seasonal patterns in the estimates of β_f and β_r for the mixed deciduous forest although sometimes the use of calcu-

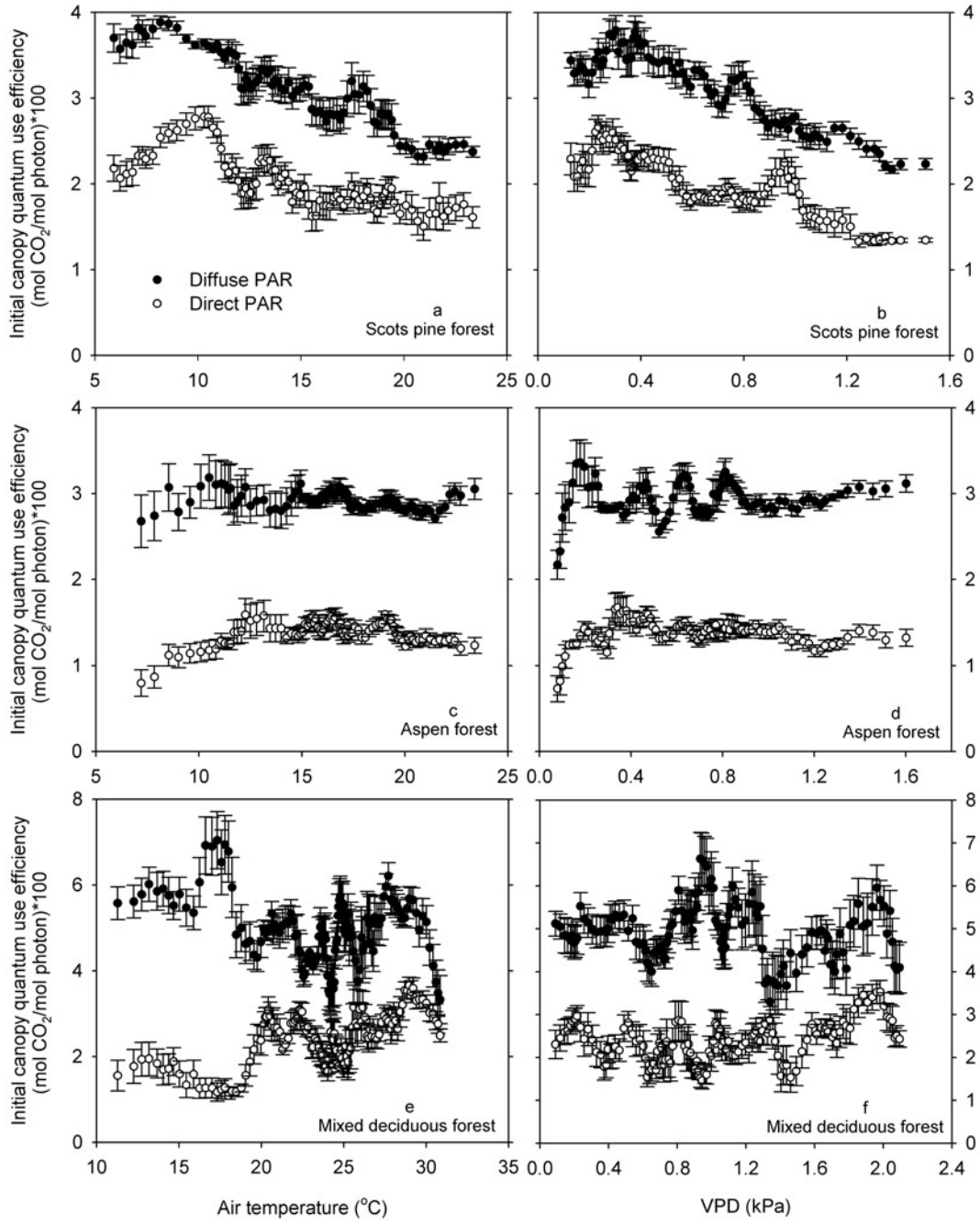

Figure 7. Responses of diffuse and direct initial canopy quantum yields α_f and α_r to changes in daily mean air temperature and VPD for the (a and b) Scots pine forest, (c and d) aspen forest, (e and f) mixed deciduous forest (using measured diffuse and direct PAR), (g and h) tallgrass prairie, and (i and j) winter wheat. Also shown are standard error bars. Data were moving-averaged.

lated values tends to decrease the differences between the estimates of β_f and β_r (Figure 8a, using measurements; Figure 8b, using calculation). Also, the sensitivity test shows that ±15% variations in the calculated diffuse PAR and accordingly direct PAR have a negligible effect on the estimates of both β_f and β_r (see Figure 8d). Therefore we feel confident that the differences between the estimated β_f and β_r reflect the differences in canopy photosynthetic effects between diffuse and direct PAR.

[54] Figure 9 plots the ratio of β_f to β_r for the five sites. Although variations of the β_f to β_r ratio are large with time and from site to site, almost all points are larger than 1. Table 5 summarizes the mean β_f, β_r and β_f to β_r ratio for the five sites. The aspen forest has both the highest mean β_f (239 μmol m^{-2} s^{-1}) and β_r (26 μmol m^{-2} s^{-1}) as well as the highest mean β_f to β_r ratio (15). The mixed deciduous forest has the smallest mean β_f (70 μmol m^{-2} s^{-1} if using measured diffuse

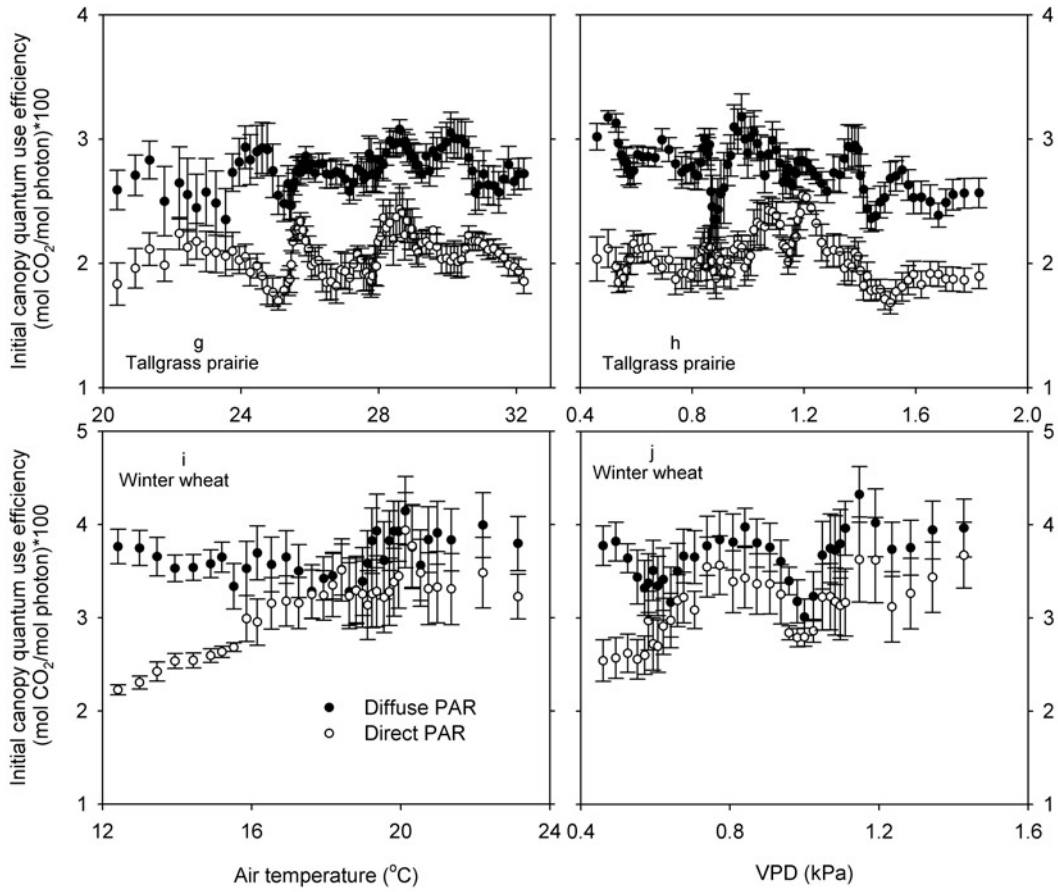

Figure 7. (continued)

and direct PAR, 64 μmol m^{-2} s^{-1} if using calculated diffuse and direct PAR) and smallest mean β_f to β_r ratio (5 if using measured diffuse and direct PAR, 4 if using calculated diffuse and direct PAR). It is interesting that while there are considerable differences in the mean values of β_f (from about 60 to 240 μmol m^{-2} s^{-1}) among the five sites, the mean values of β_r are much closer (from about 20 to 25 μmol m^{-2} s^{-1}).

4.5. Effects of Temperature and VPD on CLR Coefficients β_f and β_r

[55] Similar to what we did for α_f and α_r, we also examine how β_f and β_r change with daily mean air temperature and VPD (Figure 10). The Scots pine forest (Figure 10a), aspen forest (Figure 10c), mixed deciduous forest (Figure 10e), and winter wheat (Figure 10i) all show some levels of dependence of β_f and β_r on temperature except for the tallgrass prairie site where no clear dependence is identifiable (Figure 10g). While the β_f of the Scots pine forest tends to increase with temperature, the β_r shows the opposite trend (Figure 10a). A similar pattern is found for the aspen forest (Figure 10c). The β_r of the mixed deciduous forest tends to decrease with temperature, but the dependence of β_f on temperature appears to be nonmonotonic with the optimum temperature around 20°–25°C (Figure 10e). Both β_f and β_r of the winter wheat (Figure 10i) appear to decrease with temperature. For all five sites the responses of β_f and β_r to temperature are similar to those to VPD (Figures 10b, 10d, 10f, 10h, and 10j), again reflecting the correlation between temperature and VPD.

[56] Similar to what we observed for α_f and α_r, environmental controls on β_f and β_r do not always exhibit the same patterns. The divergence in the effects of temperature (or VPD) on β_f and β_r as revealed in Figures 10a, 10c, and 10e (or Figures 10b, 10d, and 10f) explains why sometimes out-of phase fluctuations occur in the seasonal dynamics of β_f and β_r at these sites (Figure 8). We will discuss the importance and implications of these findings later.

4.6. Effects of Light Level on the Advantages of Diffuse PAR

[57] The initial canopy quantum yields (α_f and α_r) reflect the light use efficiencies by the canopy under a "purely" diffuse or direct radiation environment when the incident light level approaches zero. As the light level increases, the canopy light use efficiency decreases because of the saturation effects. Since β_f and β_r are different, we expect that the rate of decrease in canopy light use efficiency with the light level differs between diffuse and direct PAR. Consequently, the differences in the canopy photosynthetic effects of diffuse and direct PAR change with the light level. According to Model 2, under a purely diffuse radiation environment with any light level I_f, the diffuse canopy quantum yield $\alpha_f(I_f)$ is found to be

$$\alpha_f(I_f) = \frac{\alpha_f(I_f=0)\beta_f(I_f=0)}{\alpha_f(I_f=0)+\beta_f(I_f=0)I_f} = \frac{\alpha_f\beta_f}{\alpha_f+\beta_f I_f}. \quad (9)$$

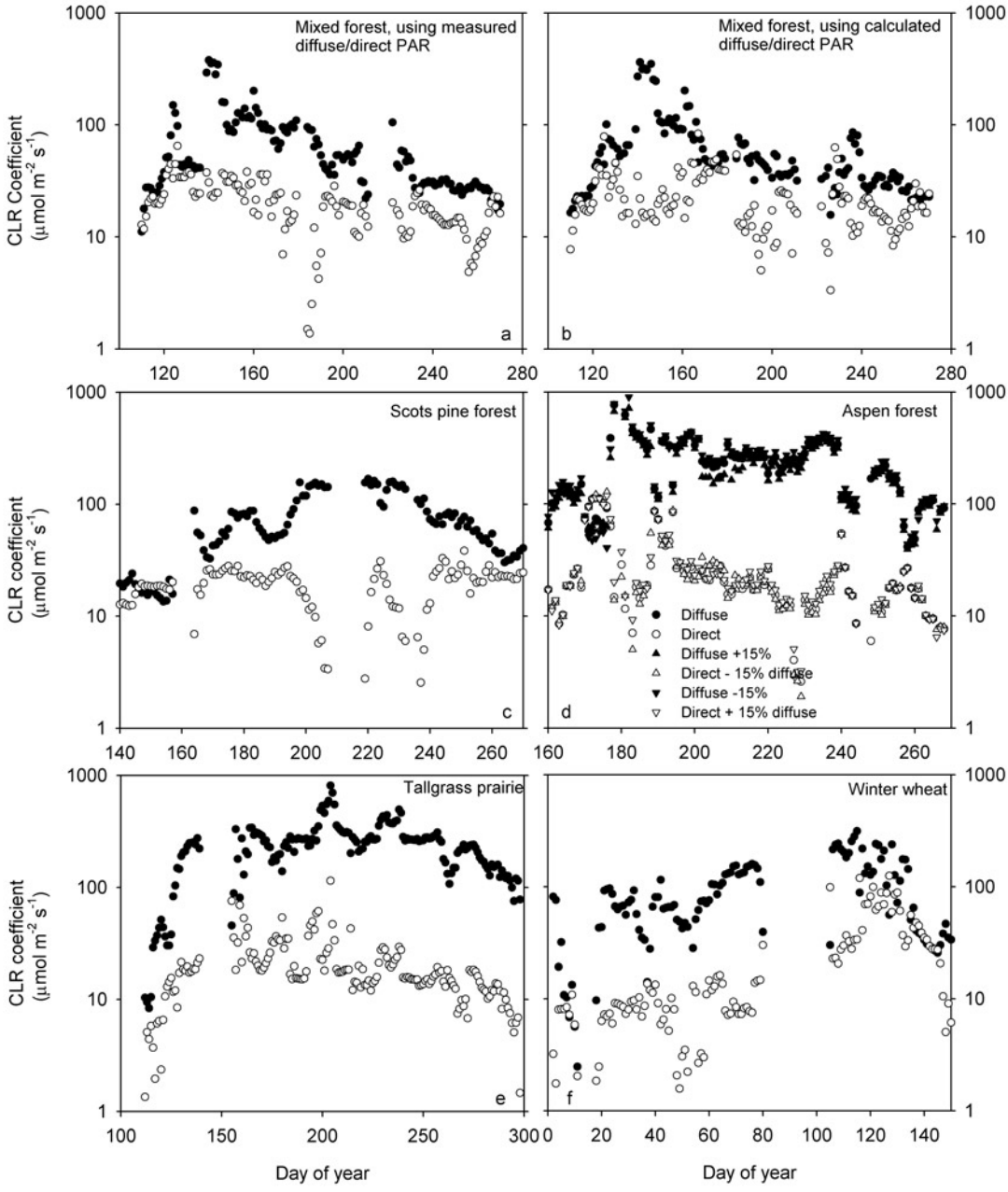

Figure 8. Seasonal dynamics of diffuse and direct CLR coefficients β_f and β_r for the mixed deciduous forest using (a) measured diffuse and direct PAR and (b) calculated diffuse and direct PAR, (c) Scots pine forest, (d) aspen forest, (e) tallgrass prairie, and (f) winter wheat. The sensitivity test results are shown for the aspen forest (Figure 8d). In the sensitivity test the diffuse PAR is varied by ±15% over the calculated values, and the direct PAR is varied accordingly to keep the measured global PAR unchanged. The obtained seasonal patterns are shown along with the original calculations. For clarity, sensitivity test results for other sites are not shown. Most missing points are due to gaps in the original measurements. A few are due to unsuccessful convergence in the regression.

A similar expression can be found for the direct canopy quantum yield at any light level I_r under a purely direct radiation environment. Now let us assume $I_f = I_r = I$ and obtain the ratio:

$$\frac{\alpha_f(I)}{\alpha_r(I)} = \frac{\alpha_f\beta_f(\alpha_r + \beta_r I)}{(\alpha_f + \beta_f I)\alpha_r\beta_r}. \quad (10)$$

Using the mean values of α_f, α_r, β_f, and β_r given in Table 5, we examine how the above ratio changes with the light level I, either purely diffuse or purely direct (Figure 11). All five sites show that the ratio $\alpha_f(I)/\alpha_r(I)$ increases almost linearly with I. From Figure 11 it is clear that it is necessary to examine both α and β simultaneously for the differences in radiation use efficiencies

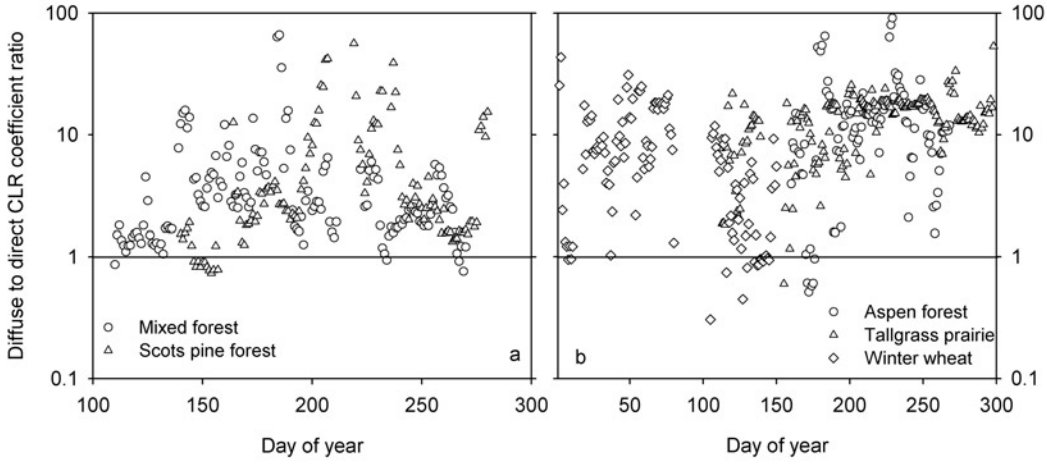

Figure 9. Ratios of diffuse to direct CLR coefficients β_f/β_r for the (a) mixed deciduous forest (using measured diffuse/direct PAR) and Scots pine forest and (b) aspen forest, tallgrass prairie, and winter wheat.

between diffuse and direct radiation since radiation use efficiencies change with radiation level.

5. Discussion and Conclusions

[58] Using tower flux measurements, we demonstrated the advantages of diffuse PAR over direct PAR for forcing canopy photosynthesis for five vegetation sites, covering a broad ecosystem spectrum and climate conditions. We found that (1) diffuse radiation results in higher light use efficiencies by plant canopies; (2) diffuse radiation has a much less tendency to cause canopy photosynthetic saturation; (3) the advantages of diffuse radiation over direct radiation increase with radiation level; (4) temperature as well as vapor pressure deficit can cause different responses in diffuse and direct canopy photosynthesis, indicating that their impacts on terrestrial ecosystem carbon assimilation may depend on radiation regimes and thus sky conditions.

[59] These findings have implications for studies of the global carbon cycle. To explain recently observed increases in photosynthetic activities in the Northern Hemisphere, researchers have been looking at nitrogen deposition, CO_2 fertilization, global warming, reforestation, and regrowth of secondary forests for answers [*Keeling et al.*, 1996; *Myneni et al.*, 1997; *Fan et al.*, 1998]. The findings in this study highlight the necessity of examining yet another factor for temporal variations of carbon sequestration in the Northern Hemisphere: changes in cloudiness and aerosol concentration. Variations in cloudiness and aerosol concentration not only change the total solar radiation at the Earth surface but also alter the relative proportions of diffuse and direct solar irradiance. *Hollinger et al.* [1994] suggested that increased haze might have enhanced terrestrial CO_2 uptake in the northern Temperate Zone. Cloudiness has increased over broad regions of the world since the beginning of the twentieth century [*McGuffie and Henderson-Sellers*, 1988; *Henderson-Sellers*, 1989; *Abakumova et al.*, 1996; *Russak*, 1990; *Karl and Steurer*, 1990; *Angell*, 1990], while atmospheric aerosol concentration has substantially increased due to anthropogenic emissions of SO_2, for example, especially in the Northern Hemisphere [*Andreae*, 1995]. Increased cloudiness and aerosol concentration may have already altered the nature of solar radiation received at the Earth's surface. Data from the former Soviet Union showed that increases in cloudiness and atmospheric turbidity were accompanied by decreases in global solar radiation and direct beam solar radiation but increases in diffuse solar radiation [*Abakumova et al.*, 1996]. *Gilgen et al.* [1998] also reported significant decreases in solar irradiance on most continents. If the benefit of increases in diffuse solar radiation overcompensates the loss caused by decreases in direct beam solar radiation for vegetation photosynthetic activities, increased cloudiness and aerosol concentration could have enhanced carbon sequestration of terrestrial ecosystems in the Northern Hemisphere during the last several decades [*Gu et al.*, 1999; *Roderick et al.*, 2001]. Further studies are needed to clarify this issue.

[60] Traditionally, light use efficiency or radiation use efficiency at the canopy level has been considered to be independent of the directional nature of solar radiation and vegetation structure [*Monteith*, 1972, 1977; *Prince*, 1991; *Prince and Goward*, 1995; *Goetz et al.*, 1999; *Ruimy et al.*, 1999]. A fundamental assumption in this definition is that plant canopies behave like one single leaf. Under this assumption, what matters is the amount of radiation absorbed by the canopy, and how the canopy absorbs the radiation is irrelevant. Such an assumption goes against the long practice by crop scientists using leaf orientation, plant geometry, and crop canopy as indicators in their breeding programs to identify superior varieties [e.g., *Pendleton et al.*, 1968; *Yoshida*, 1972]. The results presented in this paper directly supports the modeling findings of *Norman and Arkebauer* [1991] and *Choudhury* [2000, 2001a, 2001b] that light use efficiency strongly depends on the diffuse and direct composition of the incident global PAR. Clearly, light use efficiency must be treated as a function of sky conditions. It is a challenge for the next generation of regional and global primary production models, which rely on the concept of light use efficiency, to develop new algorithms to accommodate these new findings.

[61] Another finding with important implications for global primary production studies is that the dependence of canopy quantum yields on temperature (VPD) can be complicated and is vegetation (species functional type)-specific. *Ehleringer and Pearcy* [1983] and *Ehleringer et al.* [1997] reported the leaf-level measurements of quantum yield for a number of C_3 and C_4 mononcot and dicot grass species. They found that the quantum yield of C_3 species is generally driven by photorespiration and therefore decreases with temperature while temperature has no clear effects on the quantum yield of C_4 species. However, the temperature ranges reported by *Ehleringer and Pearcy* [1983]

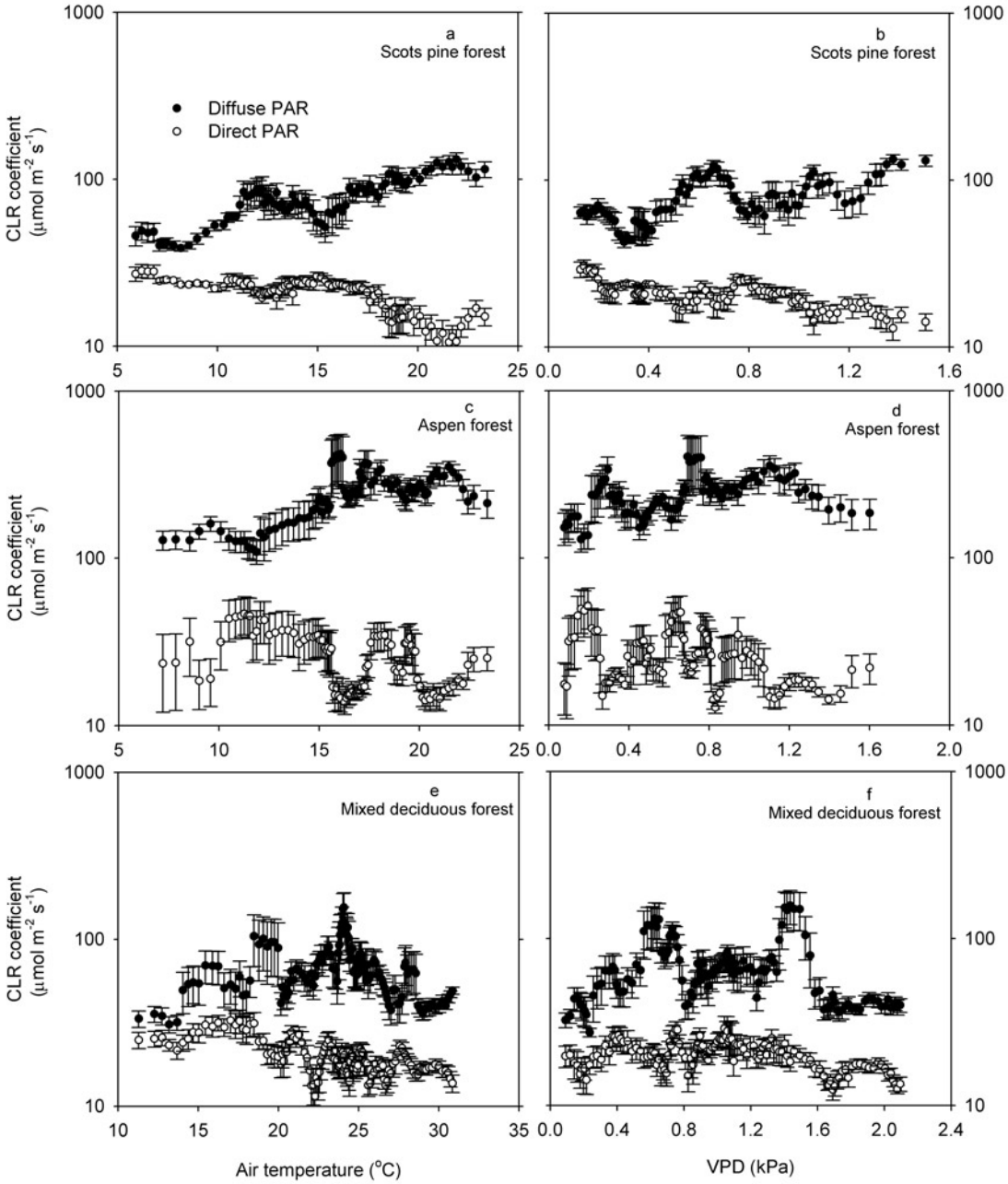

Figure 10. Responses of diffuse and direct CLR coefficients β_f and β_r to changes in daily mean air temperature and VPD for the (a and b) Scots pine forest, (c and d) aspen forest, (e and f) mixed deciduous forest (using measured diffuse and direct PAR), (g and h) tallgrass prairie, and (i and j) winter wheat. Also shown are standard error bars. Data were moving-averaged.

were mostly >15°C. Our results suggest that cautions should be taken when one generalizes the conclusions of *Ehleringer and Pearcy* [1983] and *Ehleringer et al.* [1997] to the canopy scale or extrapolates them into lower temperature ranges. The canopy quantum yields of Scots pine forest (Figure 7a), aspen forest (Figure 7c), and winter wheat crop (Figure 7i) increase with temperature when temperature is low. Nevertheless, we obtained a tendency for decrease in canopy quantum yields of the Scots pine forest with increasing temperature when temperature is larger than 10°C and no dependence for the canopy quantum yields of the tallgrass prairie. This is in agreement with *Ehleringer and Pearcy* [1983] and *Ehleringer et al.* [1997] even through the two studies worked at different scales and used different approaches.

[62] It is somewhat unexpected that impacts of temperature and VPD on the initial canopy quantum yields α_f and α_r (Figure 7) and CLR coefficients β_f and β_r (Figure 10) can diverge between diffuse and direct PAR. Obviously, this kind of phenomenon cannot happen at the leaf level. Although more studies are needed to find a sound explanation for it, we suspect that it might be related to differences in the microenvironment that sunlit and shaded leaves experience. Sunlit leaves receive not

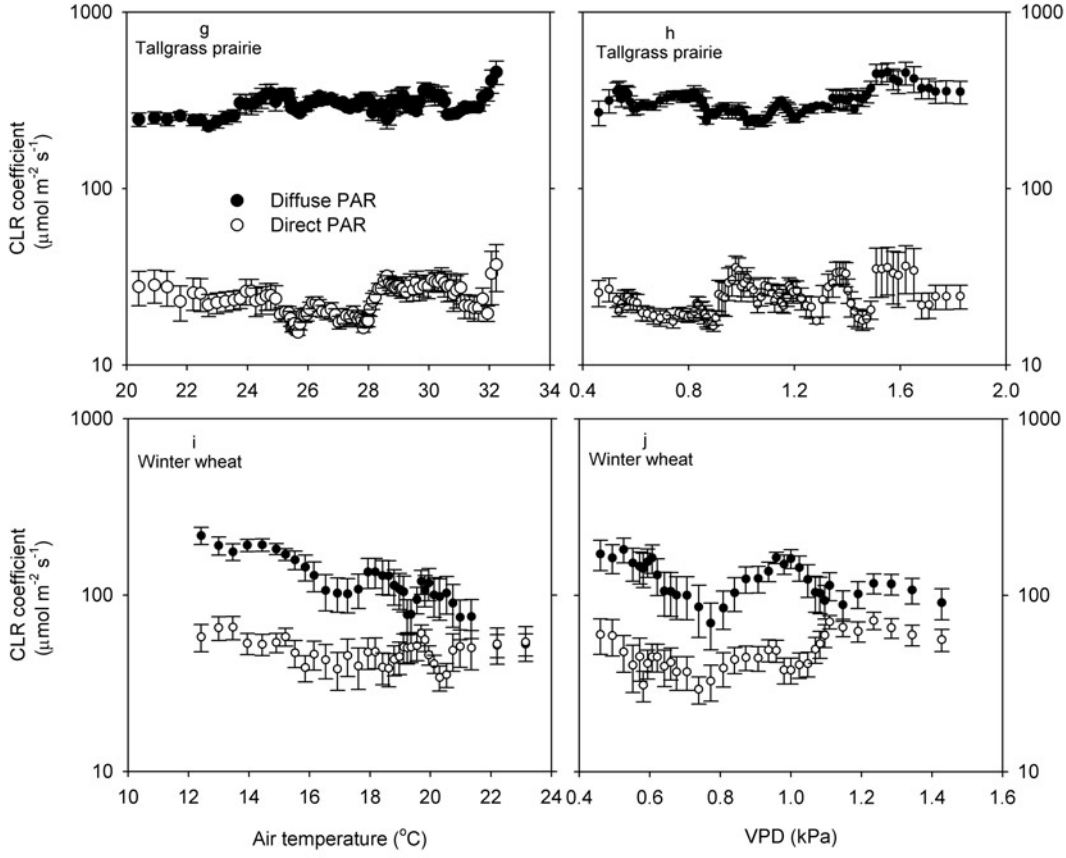

Figure 10. (continued)

only more PAR but also more near-infrared radiation than shaded leaves do. Therefore temperatures of sunlit leaves are expected to be higher than shaded leaves. This leads to greater temperature gradients between sunlit leaves and surrounding air [*Young and Smith*, 1983]. Consequently, an air temperature that is too low for shaded leaves and thus limits their photosynthetic activities might be within the right range for sunlit leaves. Conversely, an air temperature in the right range for shaded leaves might be too high and therefore limit photosynthetic activities of sunlit leaves. Differences in leaf temperature can also result in differences in VPD at the leaf surface and thus affect stomatal conductance [*Collatz et al.*, 1991; *Baldocchi*, 1997; *Baldocchi and Harley*, 1995]. Therefore responses of canopy photosynthetic parameters of diffuse and direct PAR to environmental factors may not always parallel with each other, and for certain ranges of environmental conditions divergence among diffuse and direct photosynthetic parameters can occur. The differences in environmental responses of canopy photosynthetic characteristics for diffuse and direct PAR indicate that the underlying mechanisms of terrestrial ecosystem carbon assimilation are likely a function of sky conditions. For example, we may expect that environmental controls of net ecosystem exchanges of carbon dioxide follow different patterns between cloudy and clear days.

[63] This study reiterates the conclusion of *Goudriaan* [1977] that diffuse PAR is an important variable in interpreting vegetation photosynthetic activities. Its impact depends on vegetation structure and climate conditions. However, currently diffuse PAR is not a variable commonly measured by tower flux communities. Instead, most teams measure only total PAR. As shown in this paper, a single measurement of total PAR, which masks sky conditions, hinders accurate interpretation of CO_2 flux measurements. Therefore we recommend routine measurements of diffuse radiation, particularly diffuse PAR, in tower flux measurements. In conjunction with diffuse radiation measurements, cloud observa-

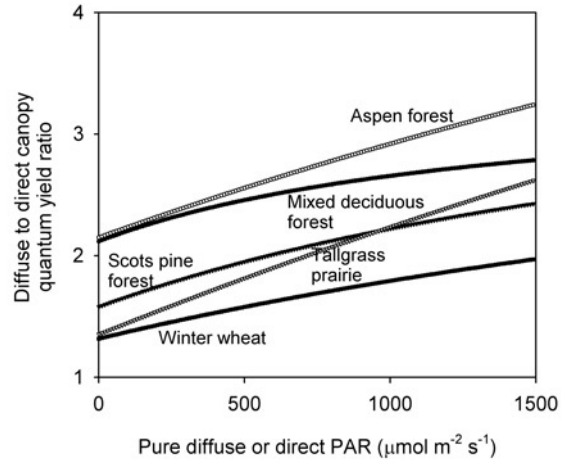

Figure 11. Changes of diffuse to direct canopy quantum yield ratio $\alpha_f(I)/\alpha_r(I)$ with the incident PAR (diffuse or direct) for the five study sites. Mean values of α_f, α_r, β_f, and β_r given in Table 5 were used in the calculation. See equation (10) and text for explanation.

tion is also desirable. By linking measured radiation components at the surface with cloud variables such as cloud cover, which may be observable from space, potential algorithms for remote sensing applications can be developed. Future generations of regional and global primary production models may use these algorithms to derive surface diffuse and direct radiation conditions from satellite observations of cloudiness to estimate terrestrial ecosystem productivities. An advantage of such a strategy is that it is applicable to all-weather conditions, including cloudy skies that current remote sensing based algorithms tend to avoid.

Appendix A: Estimating Diffuse and Direct PAR

[64] Currently, diffuse and direct PAR are not variables commonly measured by flux towers or meteorological stations. However, several models that partition measured global PAR into diffuse and direct components are available in the literature [*Goudriaan*, 1977; *Weiss and Norman*, 1985; *Spitters et al.*, 1986; *Alados and Alados-Arboledas*, 1999]. *Gu et al.* [1999] coupled several relationships published in open literature to decompose measured global PAR and solar radiation into diffuse and direct components. In this study, we adopt a similar approach. For completeness, these relationships are given here.

[65] The radiation decomposition model first computes the total diffuse (diffuse PAR plus diffuse near-infrared) fraction in global solar radiation from clearness index (k_t), solar zenith angle (θ), ambient temperature (T_a), and relative humidity (ϕ) by using relationships reported by *Reindl et al.* [1990]. Clearness index is defined as the ratio between the global solar radiation received at the Earth surface and the extraterrestrial solar radiation. The corresponding equations are [*Reindl et al.*, 1990]

Interval: $0 \le k_t \le 0.3$; constraint: $S_f/S_0 \le k_t$

$$S_f/S_0 = k_t[1 - 0.232k_t + 0.0239\cos\theta - 6.82\times10^{-4}T_a + 0.0195\phi], \quad \text{(A1a)}$$

Interval: $0.3 < k_t < 0.78$; constraint: $0.1\ k_t \le S_f/S_0 \le 0.97\ k_t$

$$S_f/S_0 = k_t[1.329 - 1.716k_t + 0.267\cos\theta - 3.57\times10^{-3}T_a + 0.106\phi], \quad \text{(A1b)}$$

Interval: $k_t \ge 0.78$; constraint: $S_f/S_0 \ge 0.1\ k_t$

$$S_f/S_0 = k_t[0.426k_t - 0.256\cos\theta + 3.49\times^{-3}T_a + 0.0734\phi], \quad \text{(A1c)}$$

where S_f denotes the total diffuse radiation received by a horizontal plane at the Earth surface ($Jm^{-2}\ s^{-1}$); S_0 denotes the extraterrestrial irradiance at a plane parallel to the Earth surface ($Jm^{-2}\ s^{-1}$), and is given by [*Spitters et al.*, 1986]

$$S_0 = S_{sc}[1 + 0.033\cos(360t_d/365)]\cos\theta, \quad \text{(A2)}$$

where S_{sc} is the solar constant (1370 J $m^{-2}\ s^{-1}$); t_d denotes the day of year.

[66] From the total diffuse radiation, diffuse PAR is calculated by using relationships reported by *Alados and Alados-Arboledas* [1999]:

$$I_f/S_f = 2.282 - 0.78\Delta + 0.067\ln\varepsilon + 0.007T_d, \quad \text{(A3)}$$

where T_d is dew point temperature (°C), I_f has the unit of (μmol $m^{-2}\ s^{-1}$), and ε and Δ are sky clearness and brightness of skylight, respectively, and are given by

$$\varepsilon = \frac{1 + (S_t - S_f)/(S_f\cos\theta) + 1.041\theta^3}{1 + 1.041\theta^3}, \quad \text{(A4)}$$

$$\Delta = S_f/S_0, \quad \text{(A5)}$$

where S_t is the global solar irradiance at the Earth surface. After diffuse PAR is obtained, direct PAR is calculated from the difference between the calculated diffuse PAR and the measured global PAR.

[67] These empirical relationships have been tested in the cited papers. We also tested the calculated diffuse and direct PAR against the 1995 measurements from the mixed deciduous forest site at Walker Branch in Tennessee, United States, and found good agreement for both diffuse and direct PAR (Figure A1).

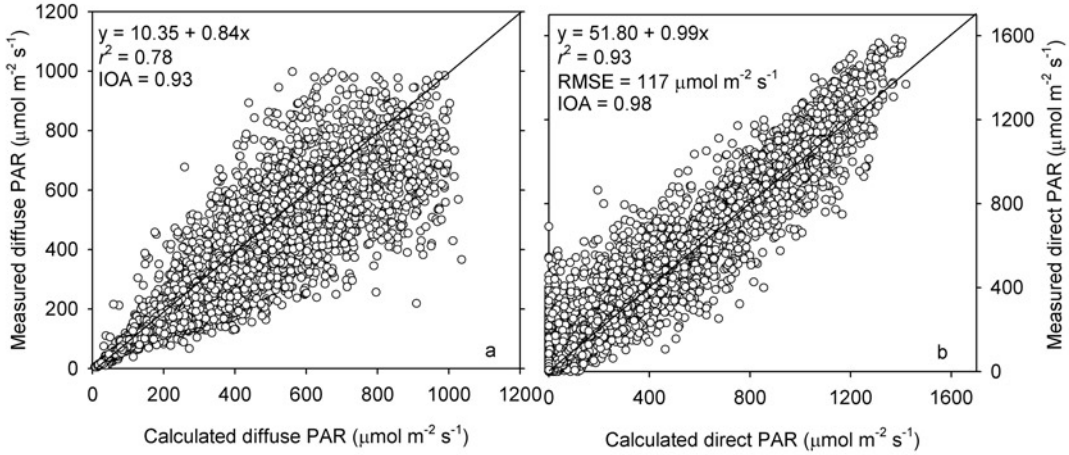

Figure A1. Relationship between measured and calculated (a) diffuse and (b) direct PAR for the mixed deciduous forest site in Walker Branch in 1995.

[68] **Acknowledgments.** This study was a contribution from the FLUXNET project sponsored by NASA's EOS Validation Program. D. D. Baldocchi received additional support for his study at the Walker Branch Watershed from the U.S. Department of Energy's Terrestrial Carbon Program. T. A. Black received support from the Climate Research Branch of the Meteorological Service of Canada, the Natural Sciences and Engineering Research Council of Canada, the Canadian Forest Service, and Parks Canada; S. B. Verma received support from the National Institute for Global Environment Change through the U.S. Department of Energy (cooperative agreement DE-FC03-90ER61010). T. Vesala received support from the European Commission, Programme Environment and Climate 1994–1998 (project EUROFLUX under contract ENV4-CT95-0078), and the Academy of Finland (project 33687); P. R. Dowty was supported through the NASA grant NAG5-7956 (Land-Surface Characterization of South African Savannas). We give special thanks to David Fitzjarrald for his critical comments on this paper. Nancy Kiang is also thanked for her helpful comments. P. T. Boggs, R. H. Byrd, J. E. Rogers, and R. B. Schnabel developed the ODRPACK package. Measurements of diffuse PAR at the Walker Branch site were obtained from the NOAA Integrated Surface Irradiance Study (ISIS) program. We thank Detlef Matt and Kell Wilson for their assistance in collecting those data.

References

Abakumova, G. M., E. M. Feigelson, V. Russak, and V. V. Stadnik, Evaluation of long-term changes in radiation, cloudiness, and surface temperature on the territory of the former Soviet Union, *J. Clim.*, *9*, 1319–1327, 1996.

Alados, I., and L. Alados-Arboledas, Direct and diffuse photosynthetically active radiation: Measurements and modeling, *Agric. For. Meteorol.*, *93*, 27–38, 1999.

Allen, L. H., D. W. Stewart, and E. R. Lemon, Photosynthesis in plant canopies: Effect of light response curves and radiation source geometry, *Photosynthtica*, *8*, 184–207, 1974.

Anderson, M. C., J. M. Norman, T. P. Meyers, and G. R. Diak, An analytical model for estimating canopy transpiration and carbon assimilation fluxes based on canopy light-use efficiency, *Agric. For. Meteorol.*, *101*, 265–289, 2000.

Andreae, M. O., Climatic effects of changing atmospheric aerosol levels, in *Future Climates of the World: A Modelling Perspective*, *World Surv. Climatol.*, vol. 16, edited by A. Henderson-Sellers, pp. 347–398, Elsevier Sci., New York, 1995.

Angell, J. K., Variations in United States cloudiness and sunshine duration between 1950 and the drought year of 1988, *J. Clim.*, *3*, 296–308, 1990.

Baldocchi, D. D., Measuring and modelling carbon dioxide and water vapour exchange over a temperate broad-leaved forest during the 1995 summer drought, *Plant Cell Environ.*, *20*, 1108–1122, 1997.

Baldocchi, D. D., and J. S. Amthor. Canopy photosynthesis: History, measurements and models, in *Terrestrial Global Productivity: Past, Present and Future*, edited by J. Roy, B. Saugier, and H. Mooney, pp. 9–31, Academic, San Diego, Calif., 2001.

Baldocchi, D. D., and P. C. Harley, Scaling carbon dioxide and water vapor exchange from leaf to canopy in a deciduous forest: Model testing and application, *Plant Cell Environ.*, *18*, 1157–1173, 1995.

Baldocchi, D. D., and K. B. Wilson, Modeling CO_2 and water vapor exchange of a temperate broad-leaved forest across hourly to decadal timescales, *Ecol. Modell.*, *142*, 155–184, 2001.

Baldocchi, D. D., B. B. Hicks, and T. P. Meyers, Measuring biosphere-atmosphere exchanges of biologically related gases with micrometeorological methods, *Ecology*, *69*, 1331–1340, 1988.

Baldocchi, D. D., C. A. Vogel, and B. Hall, Seasonal variation of carbon dioxide exchange rates above and below a boreal jackpine forest, *Agric. For. Meteorol.*, *83*, 147–170, 1997.

Baldocchi, D. D., et al., FLUXNET: A new tool to study the temporal and spatial variability of ecosystem-scale carbon dioxide, water vapor and energy flux densities, *Bull. Am. Meteorol. Soc.*, *82*, 2415–2435, 2001.

Black, T. A., et al., Annual cycles of water vapour and carbon dioxide fluxes in and above a boreal aspen forest, *Global Change Biol.*, *2*, 219–230, 1996.

Black, T. A., W. J. Chen, A. G. Barr, M. A. Arain, Z. Chen, Z. Nesic, E. H. Hogg, H. H. Neumann, and P. C. Yang, Increased carbon sequestration by a boreal deciduous forest in years with a warm spring, *Geophys. Res. Lett.*, *27*, 1271–1274, 2000.

Blanken, P. D., T. A. Black, P. C. Yang, H. H. Neumann, Z. Nesic, R. Staebler, G. Den Hartog, M. D. Novak, and X. Lee, Energy balance and canopy conductance of a boreal aspen forest: Partitioning overstory and understory components, *J. Geophys. Res.*, *102*, 28,915–28,927, 1997.

Chen, W. J., et al., Effects of climate variability on the annual carbon sequestration by a boreal aspen forest, *Global Change Biol.*, *5*, 41–53, 1999.

Choudhury, B. J., A sensitivity analysis of the radiation use efficiency for gross photosynthesis and net carbon accumulation by wheat, *Agric. For. Meteorol.*, *101*, 217–234, 2000.

Choudhury, B. J., Modeling radiation- and carbon-use efficiencies of maize, sorghum, and rice, *Agric. For. Meteorol.*, *106*, 317–330, 2001a.

Choudhury, B. J., Estimating gross photosynthesis using satellite and ancillary data: Approach and preliminary results, *Remote Sens. Environ.*, *75*, 1–21, 2001b.

Collatz, G. J., J. T. Ball, C. Grivet, and J. A. Berry, Physiological and environmental regulation of stomatal conductance, photosynthesis and transpiration: A model that includes a laminar boundary layer, *Agric. For. Meteorol.*, *54*, 107–136, 1991.

De Pury, D. G. G., and G. D. Farquhar, Simple scaling of photosynthesis from leaves to canopies without the errors of big-leaf models, *Plant Cell Environ.*, *20*, 537–557, 1997.

De Pury, D. G. G., and G. D. Farquhar, A commentary on the use of a sun/shade model to scale from the leaf to canopy, *Agric. For. Meteorol.*, *95*, 257–260, 1999.

de Wit, C. T., Photosynthesis of leaf canopies, 57 pp., Cent. for Agric. Publ. and Doc., Wageningen, Germany, 1965.

Ehleringer, J., and R. W. Pearcy, Variation in quantum yield for CO_2 uptake among C_3 and C_4 plants, *Plant Physiol.*, *73*, 555–559, 1983.

Ehleringer, J., T. E. Cerling, and B. R. Helliker, C_4 photosynthesis, atmospheric CO_2, and climate, *Oecologia*, *112*, 285–299, 1997.

Fan, S. M., S. C. Wofsy, P. S. Bakwin, and D. J. Jacob, Atmosphere-biosphere exchange of CO_2 and O_3 in the central Amazon forest, *J. Geophys. Res.*, *95*, 16,851–16,864, 1990.

Fan, S. M., M. L. Goulden, J. W. Munger, B. C. Daube, P. S. Bakwin, S. C. Wofsy, J. S. Amthor, D. R. Fitzjarrald, K. E. Moore, and T. R. Moore, Environmental controls on the photosynthesis and respiration of a boreal lichen woodland: A growing season of whole-ecosystem exchange measurements by eddy correlation, *Oecologia*, *102*, 443–452, 1995.

Fan, S., M. Gloor, J. Mahlman, S. Pacala, J. Sarmiento, T. Takahashi, and P. Tans, A large terrestrial carbon sink in North America implied by atmospheric and oceanic carbon dioxide data and models, *Science*, *282*, 442–446, 1998.

Farquhar, G. D., S. von Caemmerer, and J. A. Berry, A biochemical model of photosynthetic CO_2 assimilation in leaves of C_3 species, *Planta*, *149*, 78–90, 1980.

Fitzjarrald, D. R., K. E. Moore, R. K. Sakai, and J. M. Freedman, Assessing the impact of cloud cover on carbon uptake in the northern boreal forest (abstract), *Eos Trans. AGU*, *76*(17), Spring Meet. Suppl., S125, 1995.

Freedman, J. M., D. R. Fitzjarrald, K. E. Moore, and R. K. Sakai, Boundary layer cloud climatology and enhanced forest-atmosphere exchange, paper presented at 23rd Conference on Agricultural and Forest Meteorology, Am. Meteorol. Soc., Albuquerque, N. M., 1998.

Freedman, J. M., D. R. Fitzjarrald, K. E. Moore, and R. K. Sakai, Boundary layer clouds and vegetation-atmosphere feedbacks, *J. Clim.*, *14*, 180–197, 2001.

Gilgen, H., M. Mild, and A. Ohmura, Means and trends of shortwave irradiance at the surface estimated from global energy balance archive data, *J. Clim.*, *11*, 2042–2061, 1998.

Goetz, S. J., S. D. Prince, S. N. Goward, M. M. Thawley, and J. Small, Satellite remote sensing of primary production: An improved production efficiency modeling approach, *Ecol. Modell.*, *122*, 239–255, 1999.

Goudriaan, J., Crop micrometeorology and a simulation study, 249 pp., Cent. for Agric. Publ. and Doc., Wageningen, Germany, 1977.

Goulden, M. L., B. C. Daube, S.-M. Fan, D. J. Sutton, A. Bazzaz, J. W. Munger, and S. C. Wofsy, Physiological responses of a black spruce forest to weather, *J. Geophys. Res.*, *102*, 28,987–28,996, 1997.

Gu, L., J. D. Fuentes, H. H. Shugart, R. M. Staebler, and T. A. Black, Responses of net ecosystem exchanges of carbon dioxide to changes in cloudiness: Results from two North American deciduous forests, *J. Geophys. Res.*, *104*, 31,421–31,434, 1999.

Gutschick, V. P., Joining leaf photosynthesis models and canopy photon-transport models, in *Photon-Vegetation Interactions—Applications in Optical Remote Sensing and Plant Ecology*, edited by R. B. Myneni and J. Ross, pp. 501–535, Springer-Verlag, New York, 1991.

Harley, P. C., and J. D. Tenhunen, Modeling the photosynthetic response of C_3 leaves to environmental factors, in *Modeling Crop Photosynthesis-From Biochemistry to Canopy*, edited by K. J. Boote and R. S. Loomis, pp. 17–39, Am. Soc. of Agron., Madison, Wis., 1991.

Healey, K. D., K. G. Rickert, G. L. Hammer, and M. P. Bange, Radiation

use efficiency increases when the diffuse component of incident radiation is enhanced, *Aust. J. Agric. Res.*, *49*, 665–672, 1998.

Henderson-Sellers, A., North American total cloud amount variations this century, *Global Planet. Change*, *1*, 175–194, 1989.

Hicks, B. B., J. J. Deluisi, and D. R. Matt, The NOAA integrated surface irradiance study (ISIS)—A new surface radiation monitoring program, *Bull. Am. Meteorol. Soc.*, *77*, 2857–2864, 1996.

Hogg, E. H., B. Saugier, J.-Y. Pontailler, T. A. Black, W. Chen, P. A. Hurdle, and A. Wu, Responses of trembling aspen and hazelnut to vapor pressure deficit in a boreal deciduous forest, *Tree Physiol.*, *20*, 725–734, 2000.

Hollinger, D. Y., F. M. Kelliher, J. N. Byers, J. E. Hunt, T. M. McSeveny, and P. L. Weir, Carbon dioxide exchange between an undisturbed old-growth temperate forest and the atmosphere, *Ecology*, *75*, 134–150, 1994.

Hollinger, D. Y., et al., Forest-atmosphere carbon dioxide exchange in eastern Siberia, *Agric. For. Meteorol.*, *94*, 123–148, 1998.

Jarvis, P. G., H. S. Miranda, and R. I. Muetzelfeldt, Modeling canopy exchanges of water vapor and carbon dioxide in coniferous forest plantations, in *The Forest-Atmosphere Interaction*, edited by B. A. Hutchison and B. B. Hicks, pp. 521–542, D. Reidel, New York, 1985.

Johnson, D. W., and R. I. Van Hook, *Analysis of Biogeochemical Cycling Processes in Walker Branch Watershed*, 401 pp., Springer-Verlag, New York, 1989.

Karl, T. R., and P. M. Steurer, Increased cloudiness in the United States during the first half of the twentieth century: Fact or fiction?, *Geophys. Res. Lett.*, *17*, 1925–1928, 1990.

Keeling, C. D., J. F. S. Chin, and T. P. Whorf, Increased activities of northern vegetation inferred from atmospheric CO_2 measurements, *Nature*, *382*, 146–149, 1996.

Lamaud, E., Y. Brunet, and P. Berbigier, Radiation and water use efficiencies of two coniferous forest canopies, *Phys. Chem. Earth*, *21*, 361–365, 1997.

Landsberg, J. J., S. D. Prince, P. G. Jarvis, R. E. McMurtrie, R. Luxmore, and B. E. Medlyn, Energy conversion and use in forests: The analysis of forest production in terms of utilization efficiency (ε), in *The Use of Remote Sensing in the Modeling of Forest Productivity at Scales From the Stand to the Globe*, edited by H. L. Gholz, K. Nakane, and H. Shimoda, Kluwer Acad., Norwell, Mass., 1995.

Law, B. E., and R. H. Waring, Remote sensing of leaf area index and radiation intercepted by understory vegetation, *Ecol. Appl.*, *4*, 272–279, 1994.

Lee, X., J. D. Fuentes, R. M. Staebler, and H. H. Neumann, Long-term observation of the atmospheric exchange of CO_2 with a temperate deciduous forest in southern Ontario, Canada, *J. Geophys. Res.*, *104*, 15,975–15,984, 1999.

Lindroth, A., A. Grelle, and A. S. and, Moren, Long-term measurements of boreal forest carbon balance reveal large temperature sensitivity, *Global Change Biol.*, *4*, 443–450, 1998.

McGuffie, K., and A. Henderson-Sellers, Is Canadian cloudiness increasing?, *Atmos. Ocean*, *26*, 608–633, 1988.

Monsi, M., and T. Saeki, Über den Lichtfaktor in den Pflanzengesellschaften und seine Bedeutung für die Stoffproduktion, *Jpn. J. Bot.*, *14*, 22–52, 1953.

Monteith, J. L., Solar radiation and productivity in tropical ecosystems, *J. Appl. Ecol.*, *9*, 747–766, 1972.

Monteith, J. L., Climate and efficiency of crop production in Britain, *Philos. Trans. R. Soc. London, Ser. B*, *281*, 277–294, 1977.

Myers, R. H., *Classical and Modern Regression With Applications*, 2nd ed., 488 pp., PWS-KENT, Boston, Mass., 1990.

Myneni, R. B., C. D. Keeling, C. J. Tucker, G. Asrar, and R. R. Nemani, Increased plant growth in the northern high latitudes from 1981-1991, *Nature*, *386*, 698–702, 1997.

Norman, J. M., Interfacing leaf and canopy light interception models, in *Predicting Photosynthesis for Ecosystem Models*, vol. 2, edited by J. D. Hesketh and J. W. Jones, pp. 49–67, CRC Press, Boca Raton, Fla., 1980.

Norman, J. M., and T. J. Arkebauer, Predicting canopy light-use efficiency from leaf characteristics, in *Modeling Plant and Soil Systems*, *Agron. Monogr.*, vol. 31, pp. 125–143, Am. Soc. of Agron., Madison, Wis., 1991.

Pendleton, J. W., G. E. Smith, S. R. Winter, and T. J. Johnston, Field investigations of the relationships leaf angle in Corn (Zea mays L.) to grain yield and apparent photosynthesis, *Agron. J.*, *60*, 422–424, 1968.

Price, D. T., and T. A. Black, Effects of short-term variation in weather on diurnal canopy CO_2 flux and evapotranspiration of a juvenile Douglas-Fir stand, *Agric. For. Meteorol.*, *50*, 139–158, 1990.

Prince, S. D., A model of regional primary production for use with coarse-resolution satellite data, *Int. J. Remote Sens.*, *12*, 1313–1330, 1991.

Prince, S. D., and S. N. Goward, Global primary production: A remote sensing approach, *J. Biogeogr.*, *22*, 815–835, 1995.

Rannik, Ü., On the surface layer similarity at a complex forest site, *J. Geophys. Res.*, *103*, 8685–8697, 1998.

Rannik, Ü., and T. Vesala, Autoregressive filtering versus linear detrending in estimation of fluxes by the eddy covariance method, *Boundary Layer Meteorol.*, *91*, 259–280, 1999.

Rannik, Ü., M. Aubinet, O. Kurbanmuradov, K. K. Sabelfeld, T. Markkanen, and T. Vesala, Footprint analysis for measurements over a heterogeneous forest, *Boundary Layer Meteorol.*, *97*, 137–166, 2000.

Ratkowsky, D. A., *Handbook of Nonlinear Regression Models*, 241 pp., Marcel Dekker, New York, 1989.

Reed, K. L., E. R. Hamerley, B. E. Dinger, and P. G. Jarvis, An analytical model for field measurements of photosynthesis, *J. Appl. Ecol.*, *13*, 925–942, 1976.

Reindl, D. T., W. A. Beckman, and J. A. Duffie, Diffuse fraction correlations, *Sol. Energy*, *45*, 1–7, 1990.

Rochette, P., R. L. Desjardins, E. Patty, and R. Lessard, Instantaneous measurements of radiation use efficiency of a maize crop, *Agron. J.*, *88*, 627–635, 1996.

Roderick, M. L., G. D. Farquhar, S. L. Berry, and I. R. Noble, On the direct effect of clouds and atmospheric particles on the productivity and structure of vegetation, *Oecologia*, *129*, 21–30, 2001.

Ross, J., *The Radiation Regime and Architecture of Plant Stands*, 391 pp., Dr. W. Junk, Norwell, Mass., 1981.

Ruimy, A., G. Dedieu, and B. Saugier, Methodology of the estimation of terrestrial net primary production from remotely sensed data, *J. Geophys. Res.*, *99*, 5263–5283, 1994.

Ruimy, A., P. G. Jarvis, D. D. Baldocchi, and B. Saugier, CO_2 flux over plant canopies and solar radiation: A review, *Adv. Ecol. Res.*, *26*, 1–63, 1995.

Ruimy, A., et al., Comparing global models of terrestrial net primary productivity (NPP): Analysis of differences in light absorption and light-use efficiency, *Global Change Biol.*, *5*, suppl. 1, 56–64, 1999.

Running, S. W., D. D. Baldocchi, D. P. Turner, S. T. Gower, P. S. Bakwin, and K. A. Hibbard, A global terrestrial monitoring network: Integrated tower fluxes, flask sampling, ecosystem modeling and EOS satellite data, *Remote Sens. Environ.*, *70*, 108–127, 1999.

Runyon, J., R. H. Waring, S. N. Goward, and J. M. Welles, Environmental limits on net primary production and light-use efficiency across the Oregon transect, *Ecol. Appl.*, *4*, 226–237, 1994.

Russak, V., Trends of solar radiation, cloudiness and atmospheric transparency during recent decades in Estonia, *Tellus, Ser. B*, *42*, 206–210, 1990.

Sakai, R. K., D. R. Fitzjarrald, K. E. Moore, and J. M. Freedman, How do forest surface fluxes depend on fluctuating light level?, paper presented at 22nd Conference on Agricultural and Forest Meteorology, Am. Meteorol. Soc., Long Beach, Calif., 1996.

Sinclair, T. R., and T. Shiraiwa, Soybean radiation-use efficiency as influenced by nonuniform specific leaf nitrogen distribution and diffuse radiation, *Crop Sci.*, *33*, 808–812, 1993.

Sinclair, T. R., C. E. Murphy, and K. R. Knoerr, Development and evaluation of simplified models for simulating canopy photosynthesis and transpiration, *J. Appl. Ecol.*, *13*, 813–829, 1976.

Sinclair, T. R., T. Shiraiwa, and G. L. Hammer, Variation in crop radiation-use efficiency with increased diffuse radiation, *Crop Sci.*, *32*, 1281–1284, 1992.

Spitters, C. J. T., Separating the diffuse and direct component of global radiation and its implications for modeling canopy photosynthesis, part II, Calculation of canopy photosynthesis, *Agric. For. Meteorol.*, *38*, 231–242, 1986.

Spitters, C. J. T., H. A. J. M. Tussaint, and J. Goudriaan, Separating the diffuse and direct component of global radiation and its implications for modeling canopy photosynthesis, part I, Components of incoming radiation, *Agric. For. Meteorol.*, *38*, 217–229, 1986.

Suyker, A. E., and S. B. Verma, Year-round observations of the net ecosystem exchange of carbon dioxide in a native tallgrass prairie, *Global. Change Biol.*, *7*, 279–289, 2001.

Verma, S. B., D. D. Baldocchi, D. E. Anderson, D. R. Matt, and R. E. Clement, Eddy fluxes of CO_2, water vapor and sensible heat over a deciduous forest, *Boundary Layer Meteorol.*, *36*, 71–91, 1986.

Vesala, T., Long-term field measurements of atmosphere-surface interactions in boreal forest combining forest ecology, micrometeorology, aerosol physics and atmospheric chemistry, *Trends Heat Mass Momentum Transfer*, *4*, 17–35, 1998.

Wang, Y. P., and P. G. Jarvis, Effect of incident beam and diffuse radiation on PAR absorption, photosynthesis, and transpiration of sitka spruce—A simulation study, *Silva Carelica*, *15*, 167–180, 1990.

Wang, Y. P., and R. Leuning, A two-leaf model for canopy conductance, photosynthesis and partitioning of available energy, I, Model description and comparison with a multiplayer model, *Agric. For. Meteorol.*, *91*, 89–111, 1998.

Wang, Y. P., and R. Leuning, Reply to a commentary on the use of a sun/

shade model to scale from the leaf to canopy by D. G. G. de Pury and G. D. Farquhar, *Agric. For. Meteorol.*, *95*, 261–265, 1999.

Wang, Y. P., R. E. McMurtrie, and J. J. Landsberg, Modelling canopy photosynthetic productivity, in *Crop Photosynthesis: Spatial and Temporal Determinants*, edited by N. R. Baker and H. Thomas, pp. 43–67, Elsevier Sci., New York, 1992.

Weir, J., The fire frequency and age mosaic of a mixed wood boreal forest, M.Sc. thesis, Univ. of Calgary, Calgary, Alberta, Canada, 1996.

Weiss, A., and J. M. Norman, Partitioning solar radiation into direct and diffuse, visible and near-infrared components, *Agric. For. Meteorol.*, *34*, 205–213, 1985.

Willmott, C. T., On the validation of models, *Phys. Geogr.*, *2*, 184–194, 1981.

Willmott, C. T., Some comments on the evaluation of model performance, *Bull. Am. Meteorol. Soc.*, *63*, 1310–1313, 1982.

Wilson, K. B., and D. D. Baldocchi, Seasonal and interannual variability of energy fluxes over a broad-leaved temperate deciduous forest in North America, *Agric. For. Meteorol.*, *100*, 1–18, 2000.

Wilson, K. B., D. D. Baldocchi, and P. J. Hanson, Spatial and seasonal variability of photosynthesis parameters and their relationship to leaf nitrogen in a deciduous forest, *Tree Physiol.*, *20*, 565–587, 2000.

Wofsy, S. C., M. L. Goulden, J. W. Munger, S.-M. Fan, P. S. Bakwin, B. C. Daube, S. L. Bassow, and F. A. Bazzaz, Net exchange of CO_2 in a midlatitude forest, *Science*, *260*, 1314–1317, 1993.

Yoshida, S., Physiological aspects of grain yield, *Ann. Rev. Plant Physiol.*, *23*, 437–464, 1972.

Young, D. R., and W. K. Smith, Effect of cloud cover on photosynthesis and transpiration in the subalpine understory species *Arnica Latifolia*, *Ecology*, *64*, 681–687, 1983.

D. Baldocchi and L. Gu, Ecosystem Science Division, Department of Environmental Science, Policy and Management, 151 Hilgard Hall, University of California, Berkeley, CA 94720-3110, USA. (lianhong@nature.berkeley.edu)

T. A. Black, Faculty of Agricultural Sciences, University of British Columbia, Vancouver, British Columbia, Canada V6T 1Z4.

P. R. Dowty, Puget Sound Water Quality Action Team, Office of the Governor, P.O. Box 40900, Olympia, WA 98504-0900, USA.

E. M. Falge, Department of Plant Ecology, University of Bayreuth, 95440 Bayreuth, Germany.

S. B. Verma, School of Natural Resource Sciences, University of Nebraska, Lincoln, NE 68583-0728, USA.

T. Vesala, Department of Physical Sciences, University of Helsinki, FIN-00014 Helsinki, Finland.